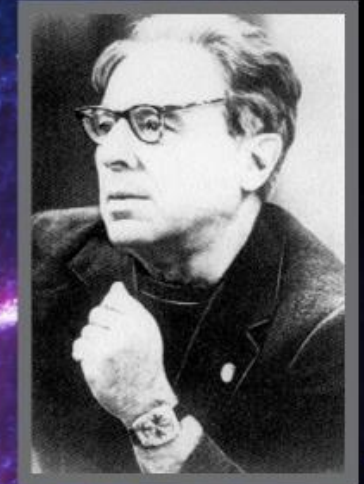


INTERNATIONAL CONFERENCE “ALL - WAVE ASTRONOMY. SHKLOVSKY - 100”.

A scientific meeting in honour of 100th anniversary of Iosif S. Shklovsky

20 - 22 June 2016, Moscow, Russia

<http://shklovsky100.asc.rssi.ru>



Topics of the conference

- Cosmic Microwave Background and the Early Universe
- Supermassive black holes and active galactic nuclei
- Sources of cosmic rays generation
- Supernovae and their remnants, gamma-ray bursts, pulsars
- Physics of the interstellar medium
- Stellar evolution and planetary systems
- The SETI problem.

Shklovskii's predictions on SN1987A

Why are there no type II supernovae in irregular galaxies?

I. S. Shklovskii

Institute for Space Research, USSR Academy of Sciences, Moscow

(Submitted March 26, 1984)

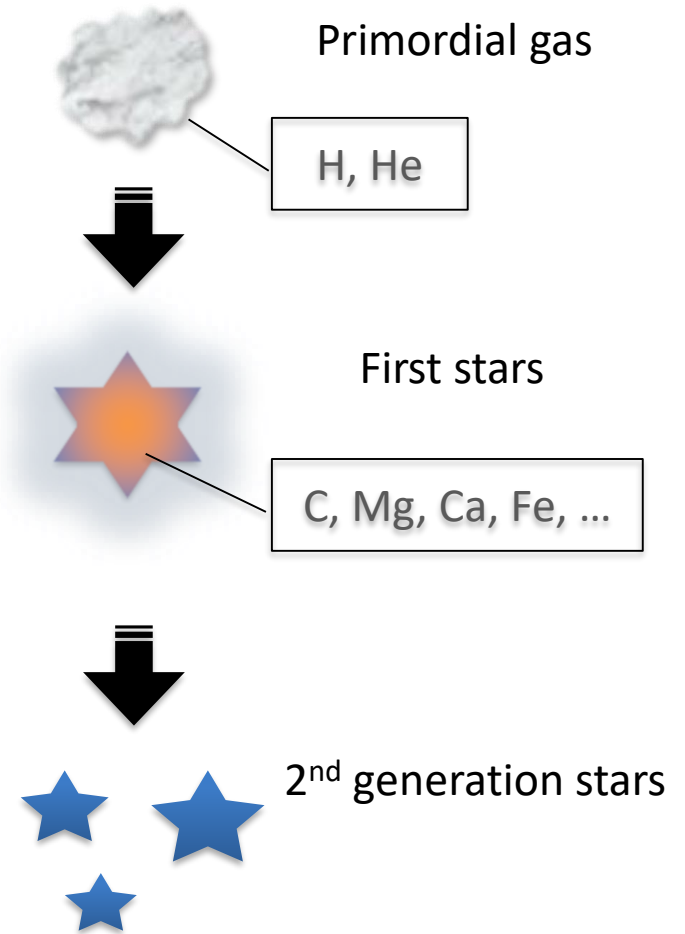
Pis'ma Astron. Zh. **10**, 723–725 (October 1984)

Irregular galaxies may lack type II supernovae because these systems are deficient in heavy elements, so that their hot, massive giants produce no observable stellar wind. Accordingly, massive stars undergoing terminal evolution will not be embedded in the dense, extended envelopes that are necessary if the SN II phenomenon is to be detected.

- Based on the theory of SN light curves, developed by V.S.Imshennik, D.K.Nadyozhin and E.K.Grasberg, Shklovskii predicted in 1984 that supernovae of type II exploding in galaxies similar to the Large Magellanic Cloud **must have low luminosity due to the relatively small radius of SNII progenitors in low metallicity environments.** This prediction was brilliantly confirmed by SN1987A.

First (Pop III) stars

- Zero metallicity stars
- Formation of the first stars: density fluctuations and gravitational contraction
- The nature is still unknown: IMF and supernova explosions

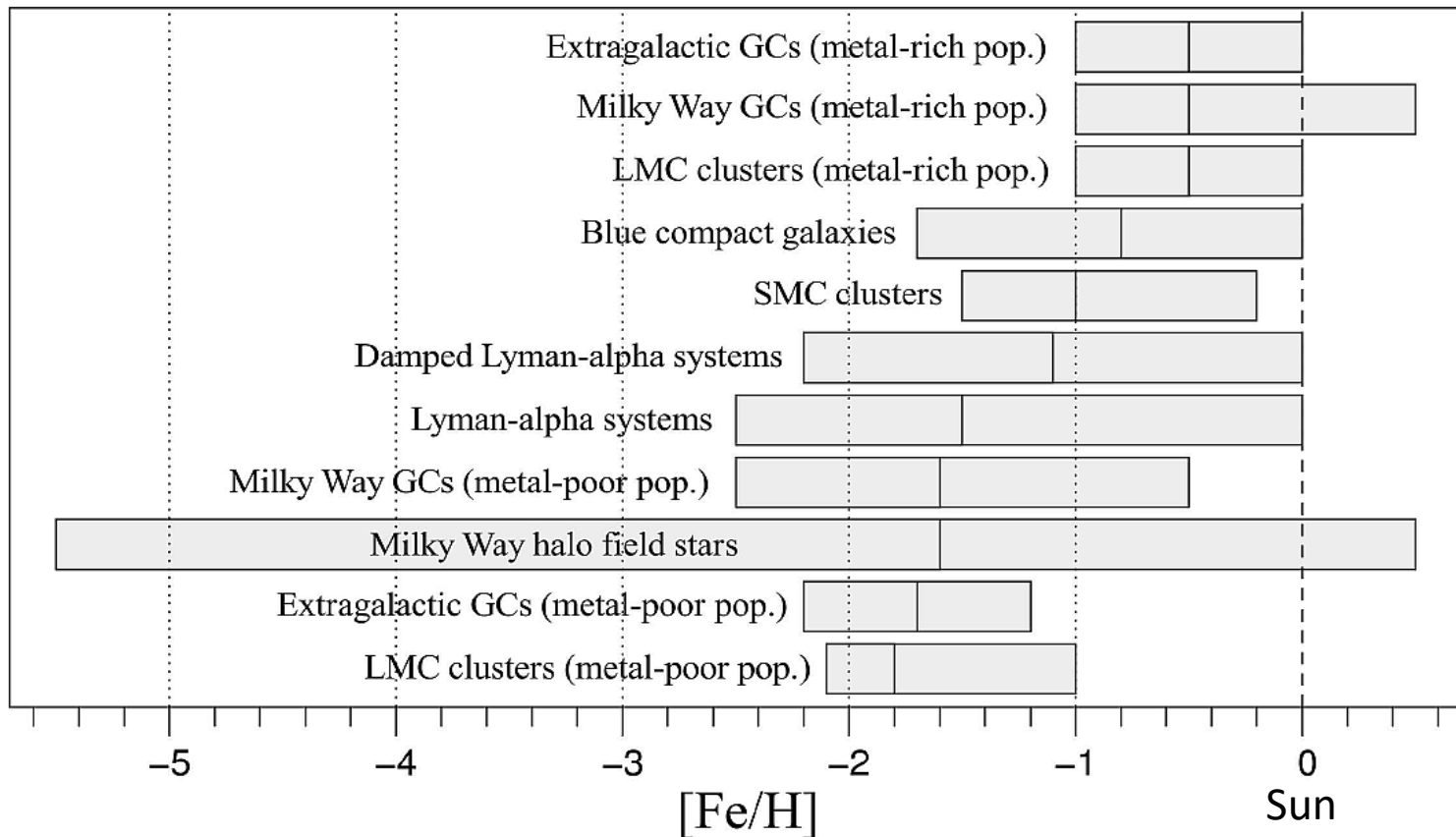


Low Metallicities in Perspective

The nature of the first stars has mainly been studied using low-mass stars in the Galactic halo.

These stars have a lifetime longer than the current age of the universe, and thus preserve the chemical abundance at the time of their formation.

Such stars are referred to as metal-poor stars.



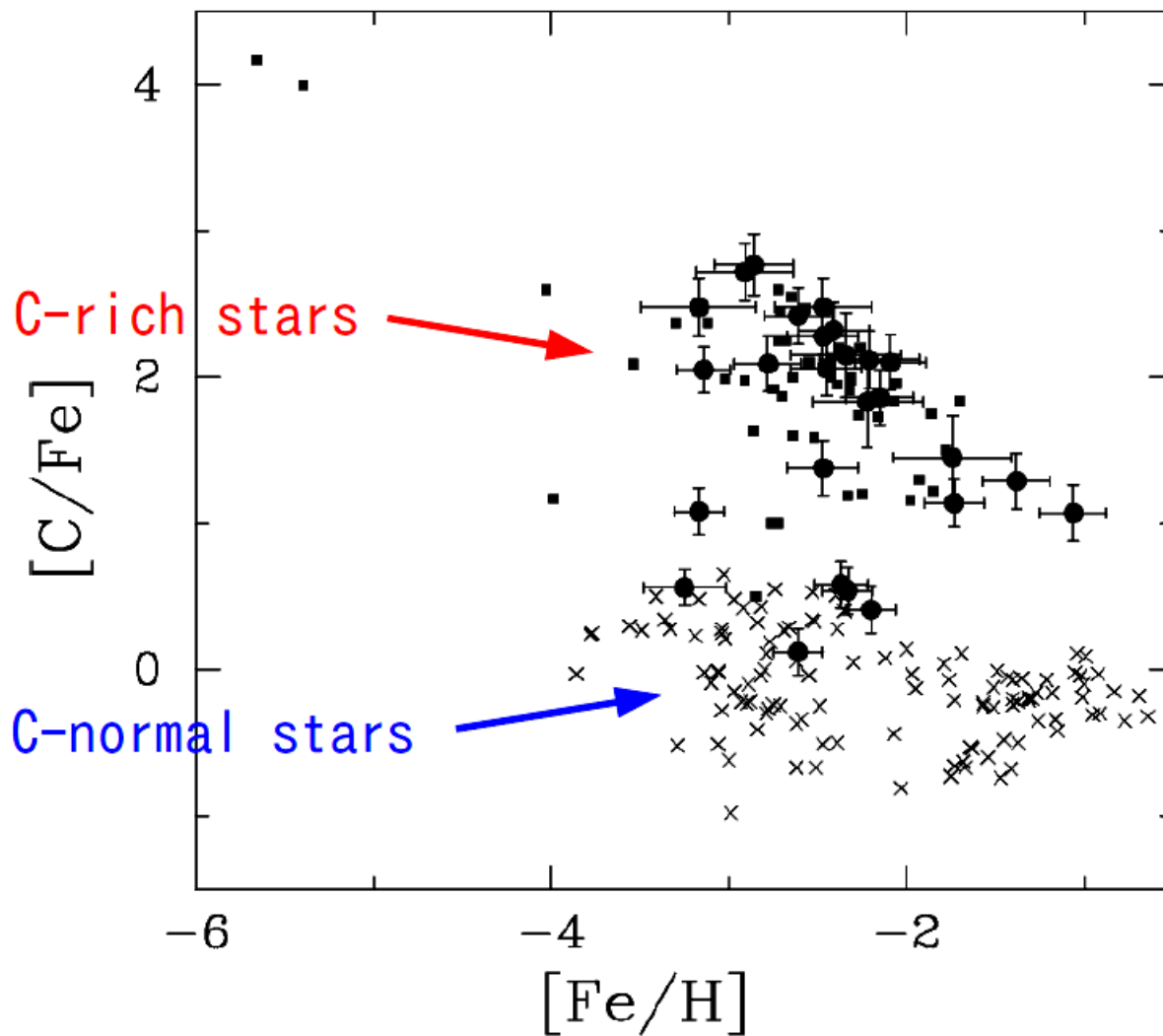
Metal poor stars

- Mega Metal Poor (MMP): $[\text{Fe}/\text{H}] < -6$
- Hyper Metal Poor (HMP): $[\text{Fe}/\text{H}] < -5$
- Ultra Metal Poor (UMP): $[\text{Fe}/\text{H}] < -4$
- Extremely Metal Poor (EMP) : $[\text{Fe}/\text{H}] < -3$
- Very Metal Poor (VMP): $[\text{Fe}/\text{H}] < -2$
- Metal Poor (MP) : $[\text{Fe}/\text{H}] < -1$
- Solar: $[\text{Fe}/\text{H}] \sim 0$
- Super Metal Rich (SMR): $[\text{Fe}/\text{H}] > +0.5$

$$[\text{Fe}/\text{H}] = \log(\text{Fe}/\text{H}) - \log(\text{Fe}/\text{H})_{\odot}$$

(Beers & Christlieb 2005)

C-abundance distribution (Takeda 2007)



In particular, all of the HMP stars show extremely high C abundance with $[C/Fe] > +3$.

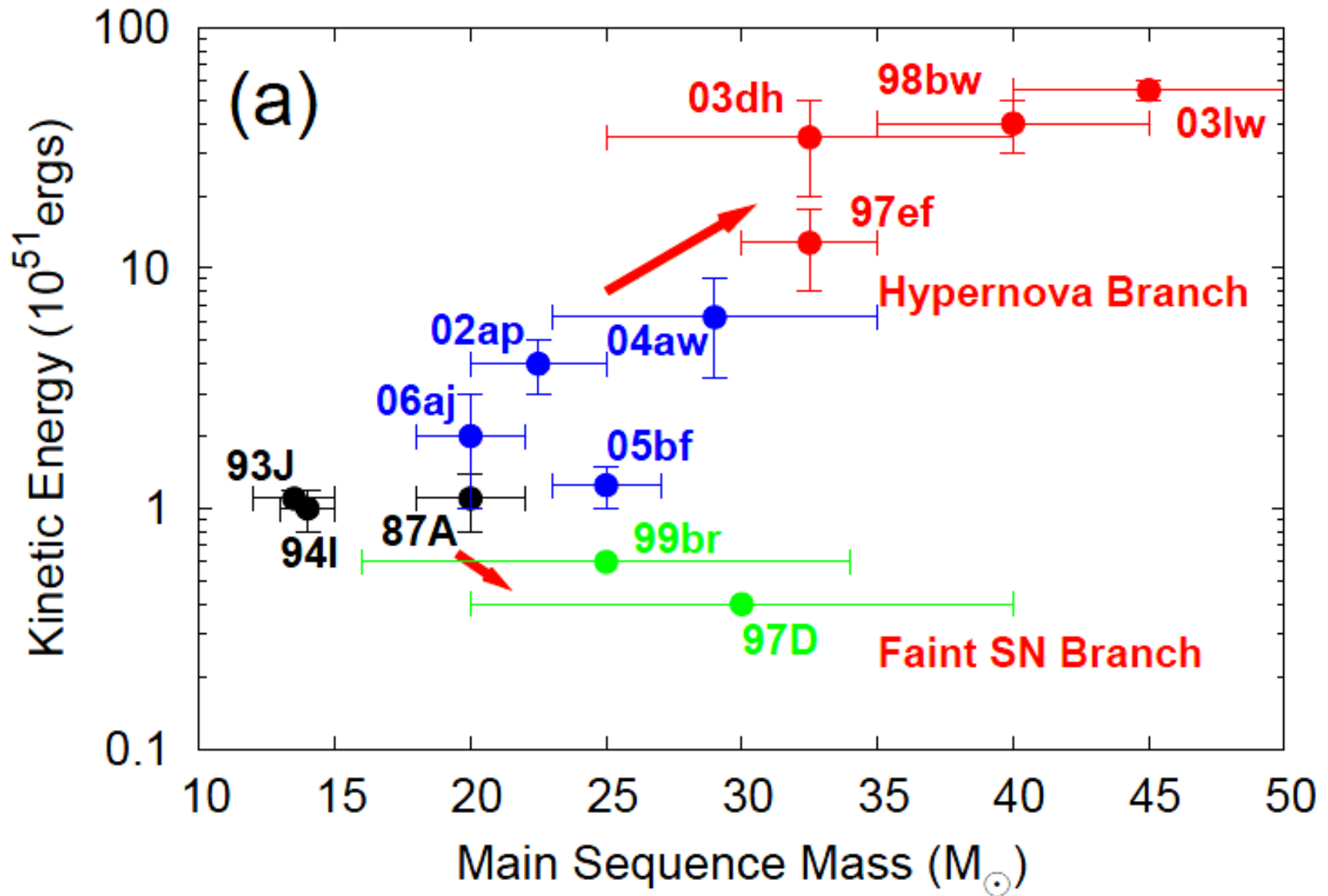
Theoretical studies

- Abundance patterns of the C-normal EMP stars are well reproduced by SN explosions with main-sequence masses M_{ms} of $< 100 M_{\odot}$.
(Umeda & Nomoto 2002; Limongi et al. 2003; Tominaga et al. 2007b, 2014a; Heger & Woosley 2010).
- For most of CEMP stars with $[\text{Fe}/\text{H}] < -3$ and for HMP stars, the C enhancements require faint SNe which eject a small mass of $^{56}\text{Ni} = 0.001\text{-}0.01 M_{\odot}$ for CEMP stars and $0.01 M_{\odot}$ for HMP stars.
(e.g., Iwamoto et al. 2005; Heger & Woosley 2010; Ishigaki et al. 2014; Tominaga et al. 2014a).

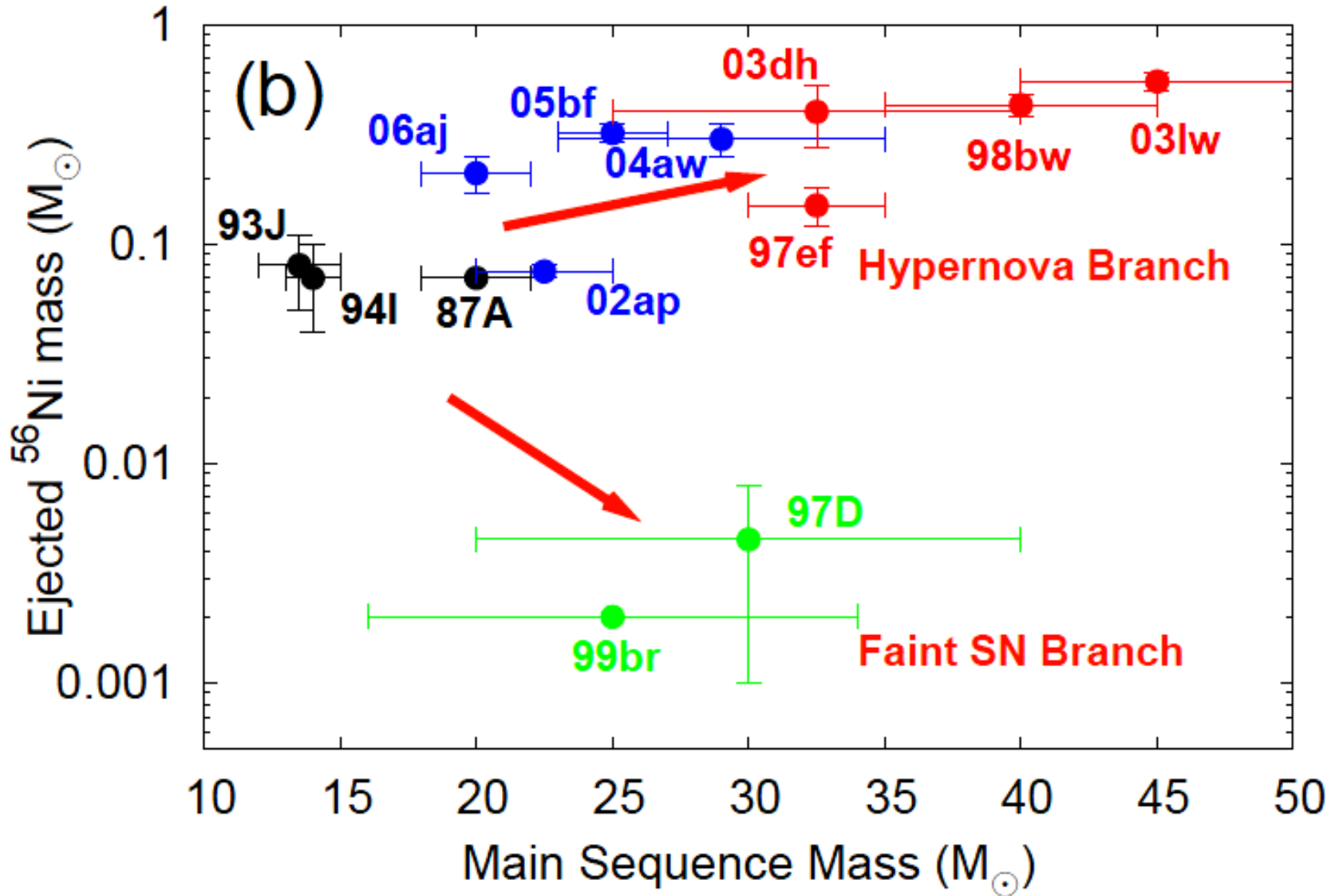
Observations

- While analogies of faint SNe for CEMP stars have been detected recently (SN 1997D and SN 1999br, SN 2008ha), the ejected ^{56}Ni masses of the faint SN models for HMP stars are smaller than those estimated from light-curve analyses of nearby observed SNe. **Non-existence of such a faint SN in the present day/selection effect in the observations of nearby SNe**
- In metal-free pockets at $z \sim 2$ (Fumagalli et al. 2011), and possible Pop III remnants at $z = 3.5$ are also observed (Crighton et al. 2015).

Explosion energy vs MS mass (Tominaga et al., 2007)



Ejected ^{56}Ni vs MS mass (Tominaga et al., 2007)



Energy scales (by A. Heger, 2010)

Log E	Explosion	Thermonuclear
39	X-ray Bursts	√
40	Long-Duration He Bursts	√
41		
42	X-ray Superbursts	√
43		
44		
45		
46	Classical Novae	√
48	Faint SN (visible LC?)	
49	SN (visible LC)	
50	Bright SN (LC?)	
51	SN (kinetic)	SN Type Ia total
52	Hypernova? GRB?	Pair-SN total (low-mass end)
53	SN (neutrinos – several 10^{53} erg)	Pair-SN total (upper limit)
54	<i>(a lot of energy - $0.5 M_{\odot} c^2$)</i>	
55	GR He SN	GR He SN (upper limit)
56	GR H SN, $Z > 0$ (Fuller <i>et al.</i> 1986)	√

Context/Aims

- No detection of Pop III stars and their SN)explosions
- Many transient surveys are conducted and the feasibility of the detection is growing (KISS,PTF, ASSASN and Subaru/HSC,LSST)
- We study the multicolor light curves for a number of metal-free core-collapse supernova models (25-100 Msun) to determine the indicators for the detection and identification of first generation SNe.
- Unlike similar numerical simulations performed by Whalen et al. (2013) and Smidt et al. (2014), we mostly concentrate on realistic SN models that reproduce the observed abundance patterns of metal-poor stars (Ishigaki et al. 2014).

Z0 and Zsolar Models

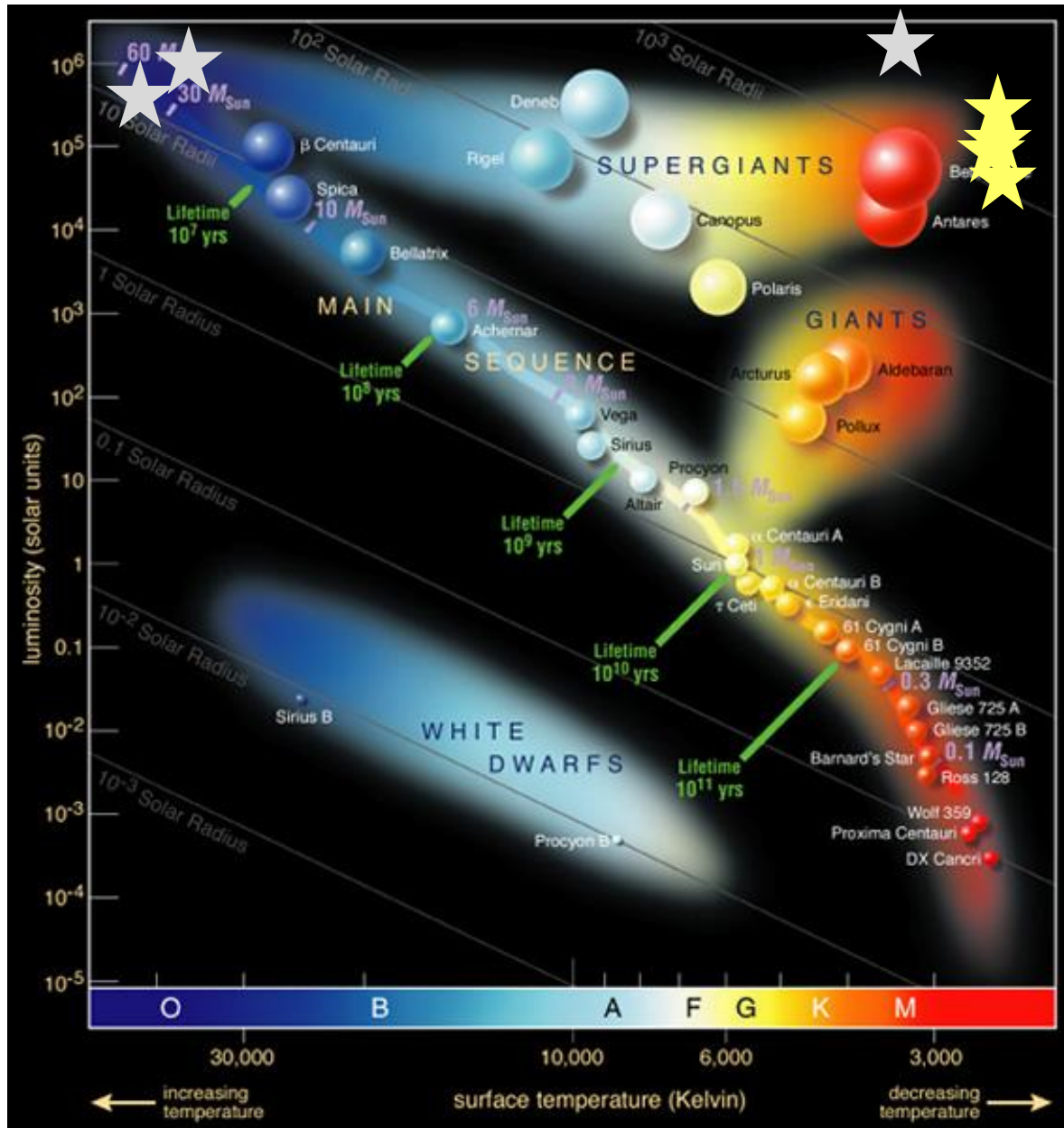


Table 1
Zero metallicity explosion models

Model	Z	M [M_{\odot}]	T_c [$10^3, K$]	Luminosity [$10^6, L_{\odot}$]	Radius [R_{\odot}]	M(H) [M_{\odot}]	Energy [E_{51}]	$M_{\text{cut}}(\text{ini})$ [M_{\odot}]	$M_{\text{mix}}(\text{out})$ [M_{\odot}]	M(^{56}Ni) [M_{\odot}]	[C/Fe]*
25z0E1	0	25	40	0.32	30	11.1	1	-	1.7	0.2	0.9
25z0E1M								1.7	5.7	0 ... 10^{-2}	1.9
25z0E10							10	-	1.6	0.7	0.3
25z0E10M								1.7	6.4	0 ... 10^{-1}	0.5
40z0E1M	0	40	27	0.88	85	15.0	1.3	2.0	12.7	0 ... 10^{-1}	0.6
40z0E30							30	-	2.0	0.8	0.4
40z0E30M1								2.0	5.5	0 ... 10^{-1}	1.3
40z0E30M2								2.5	14.3	0 ... 10^{-1}	0.1
100z0E1M	0	100	3.5	2.2	2200	27.1	2.0	2.0	40	0 ... 10^0	0.6
100z0E60							60	-	2.3	5.2	0.03
100z0E60M								2.3	40	0 ... 10^0	-0.3

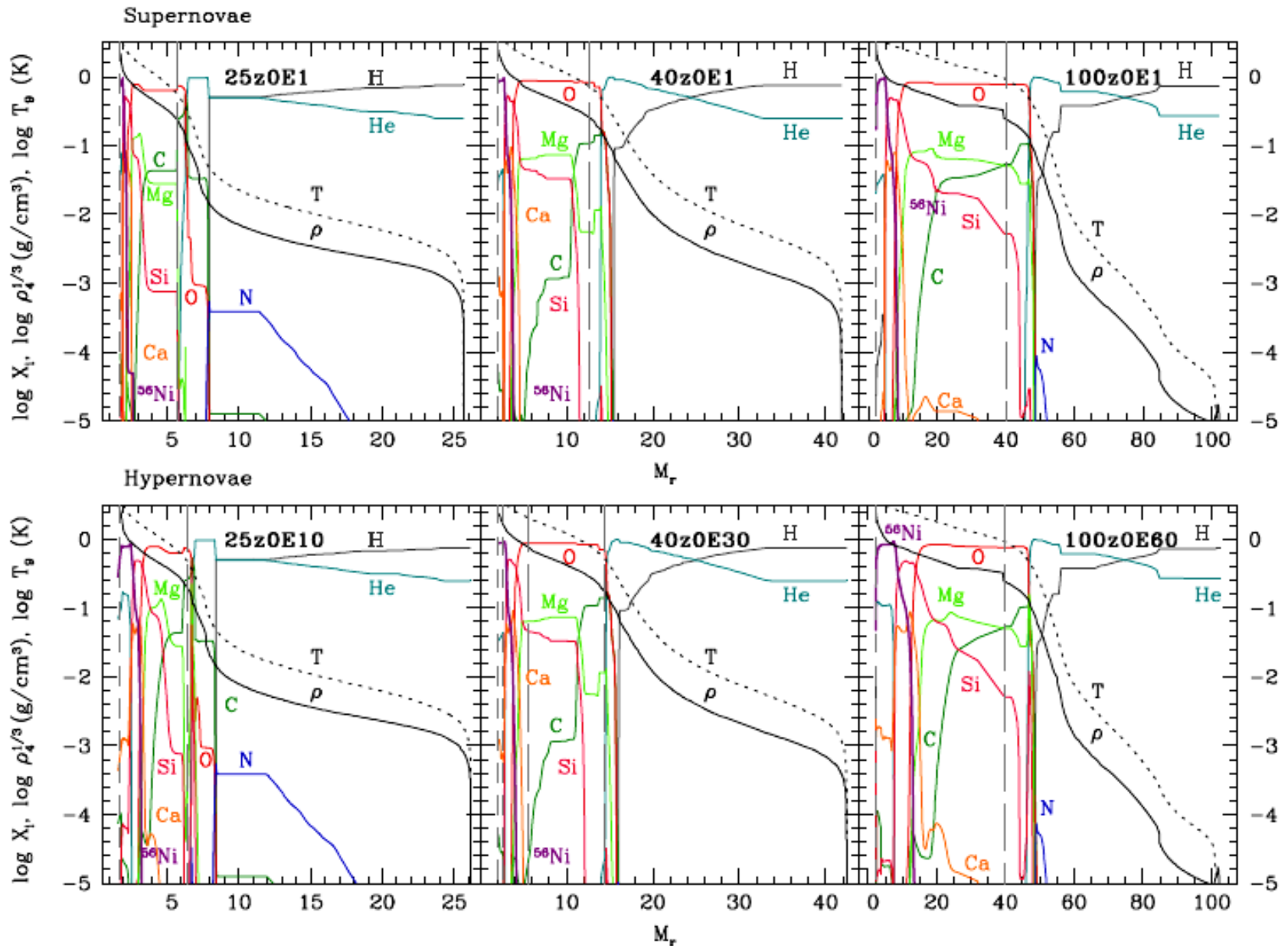
Note. — The numbers shown are metallicity, main-sequence mass, color temperature, luminosity, radius, hydrogen mass, explosion energy, mixing-fallback inner and outer mass, ^{56}Ni mass, **carbon-to-iron ratio**
* For mixing-fallback models the value for the models with highest amount of ^{56}Ni is shown.

Table 2
Non-zero metallicity explosion models

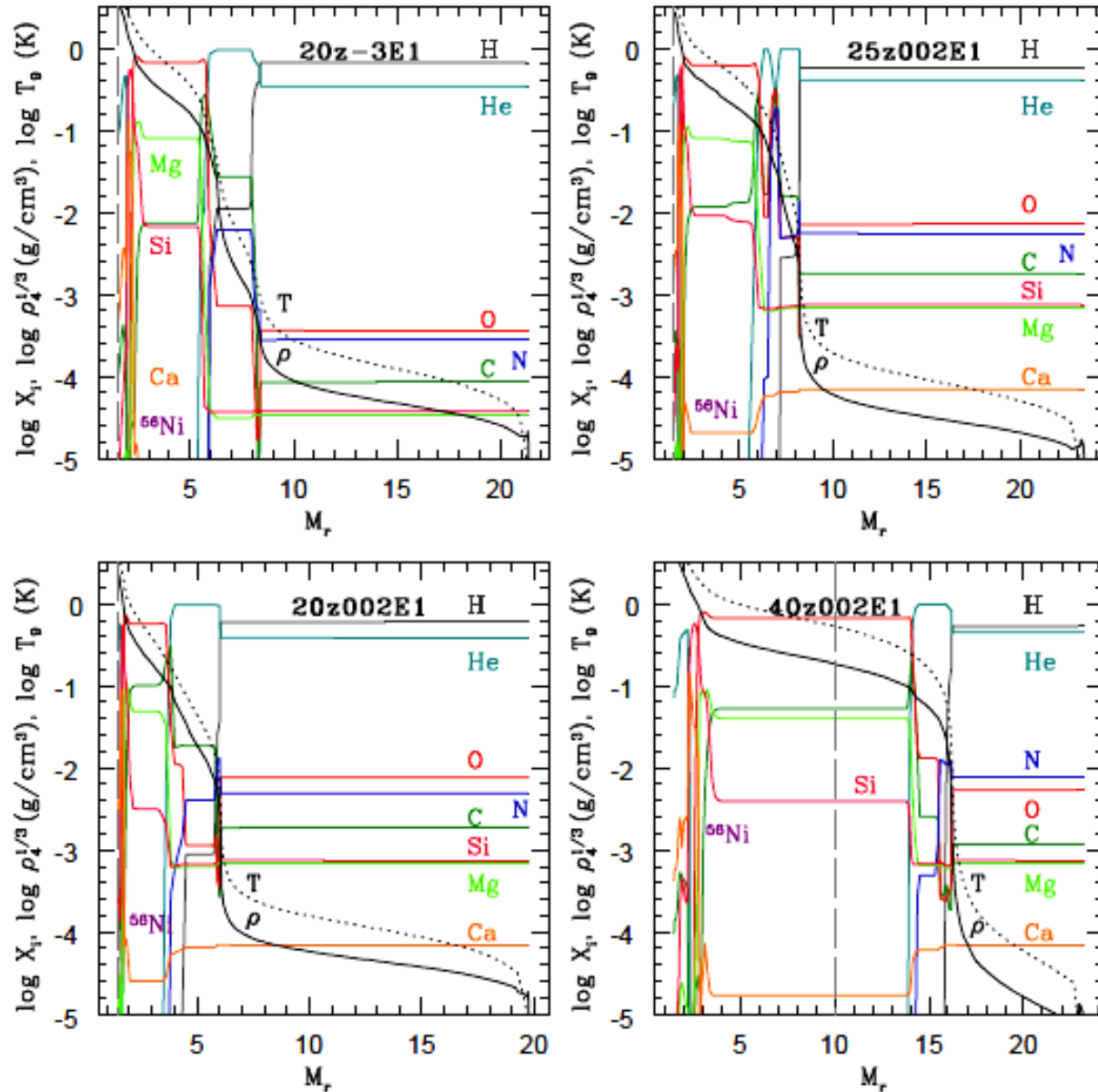
Model	Z	M [M_{\odot}]	T_c [$10^3, K$]	Luminosity [$10^6, L_{\odot}$]	Radius [R_{\odot}]	M(H) [M_{\odot}]	Energy [E_{51}]	M_{cut} [M_{\odot}]	M(^{56}Ni) [M_{\odot}]
20z-3E1	0.001	20 (20)	2.6	0.12	760	8.7	1	1.5	0; 0.4
20z002E1	0.02	20 (18)	2.4	0.08	800	8.2	1	1.5	0; 0.1
25z002E1	0.02	25 (22)	2.4	0.17	1200	8.7	1	1.5	0; 0.24
25z002E1M	0.02	25 (18)	2.4	0.17	1200	8.7	1	1.7-5.7*	0; 10^{-3} ; 0.1
40z002E1	0.02	40 (22)	2.5	0.55	1700	3.7	1	10.0	0

Note. — The numbers shown are metallicity, main-sequence mass (presupernova mass), color temperature, luminosity, radius, hydrogen mass, explosion energy, mass cut, mixing-fallback inner and outer mass, ^{56}Ni mass. By * mixing-fallback parameters are indicated: $M_{\text{cut}}(\text{ini})$, $M_{\text{mix}}(\text{out})$.

z0 presupernova composition and structure



z002 presupernova composition and structure



Mixing-fallback model (Tominaga et al., 2007)

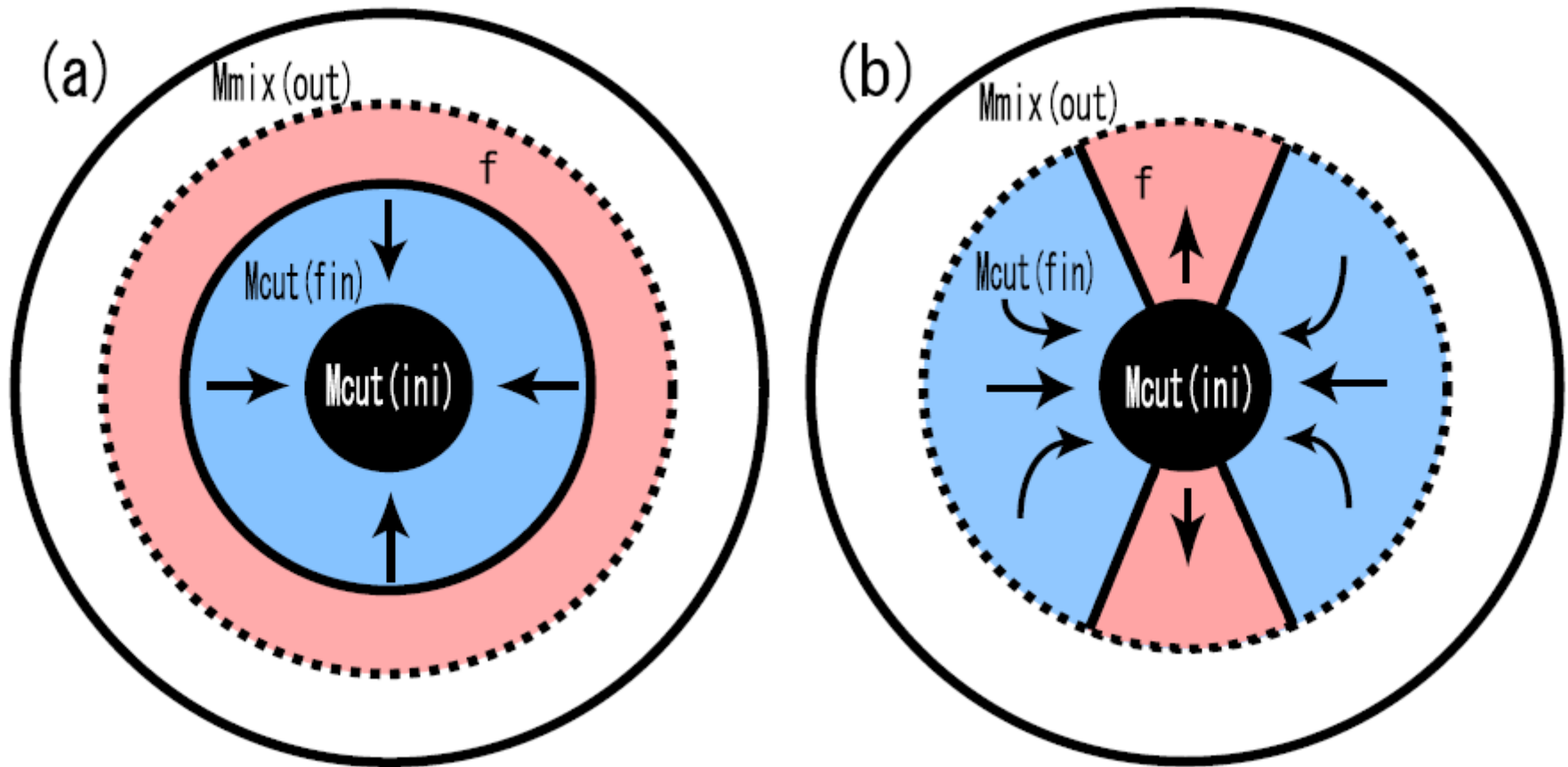
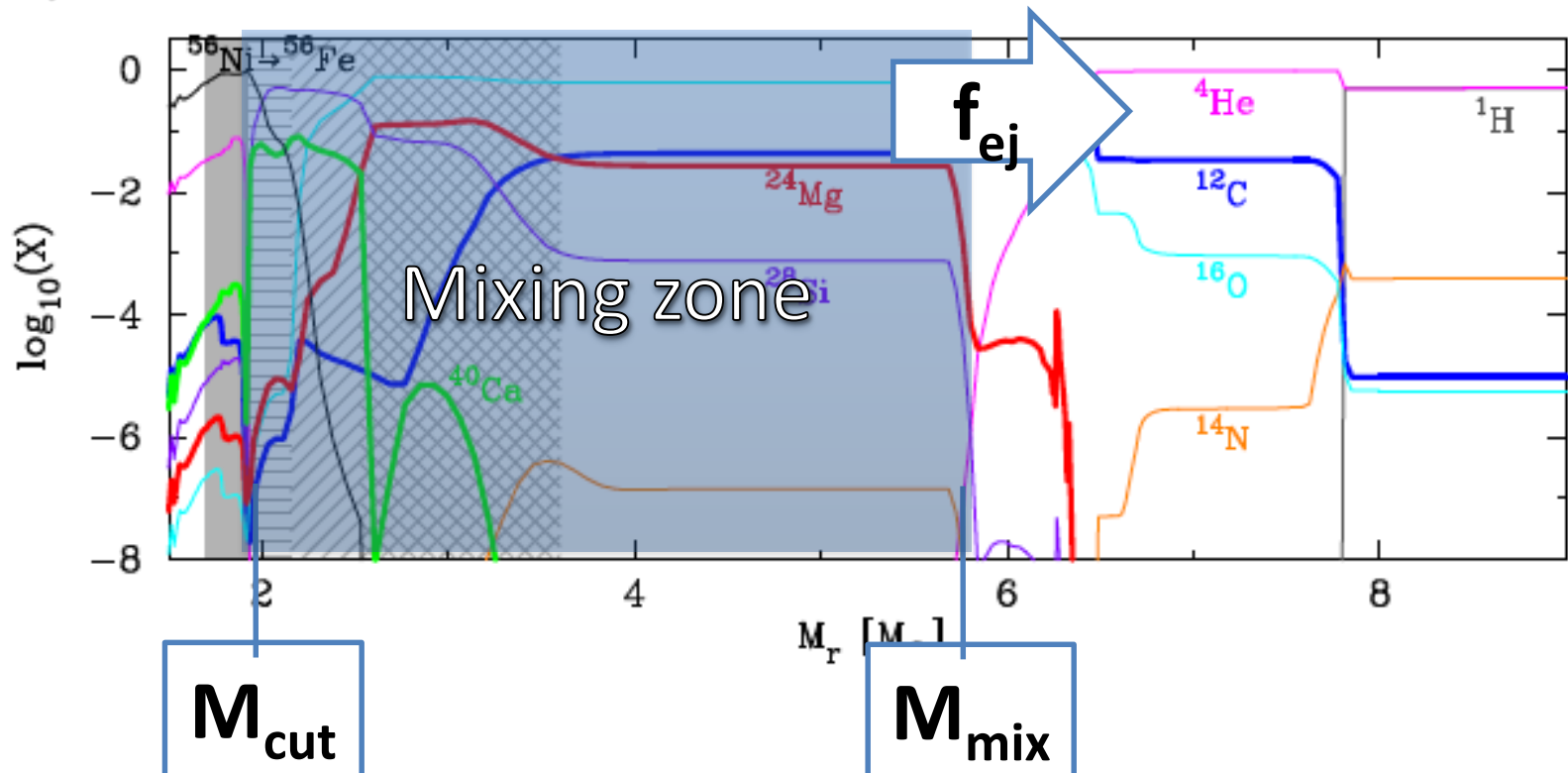


Fig. 12.— The illustration of the mixing-fallback model. The central black region is the initial mass cut, that is, inside the inner boundary of the mixing region, $M_{\text{cut}}(\text{ini})$. The mixing region is enclosed with the dotted line. A fraction f of the materials in the mixing region ejected to the interstellar space. The rest materials, locating in the blue region, fallback into the central remnant. (a) 1-dimensional picture. The materials mixed up to a given radius, and a part of the materials are ejected. (b) 2-dimensional picture. While the all materials in the outer region above $M_{\text{mix}}(\text{out})$, are ejected, the materials in the mixing region may be ejected only along the jet-axis. In the jet-like explosion, the ejection factor f depends on the jet-parameters (e.g., an opening angle and an energy deposition rate).

Mixing-fallback model (by Ishigaki)

- Mixing-fallback parametrization (Tominaga et al. 2007)
 - $M_{\text{cut}}(\text{ini})$: Inner boundary of mixing
 - $M_{\text{mix}}(\text{out})$: Outer boundary of mixing
 - f_{ej} : ejected fraction (fraction of mass ejected in the mixing zone)

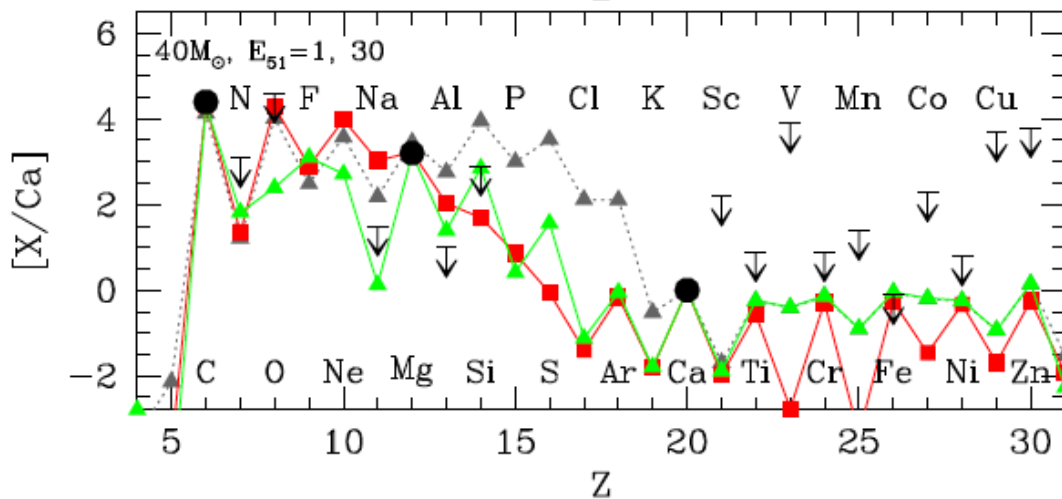
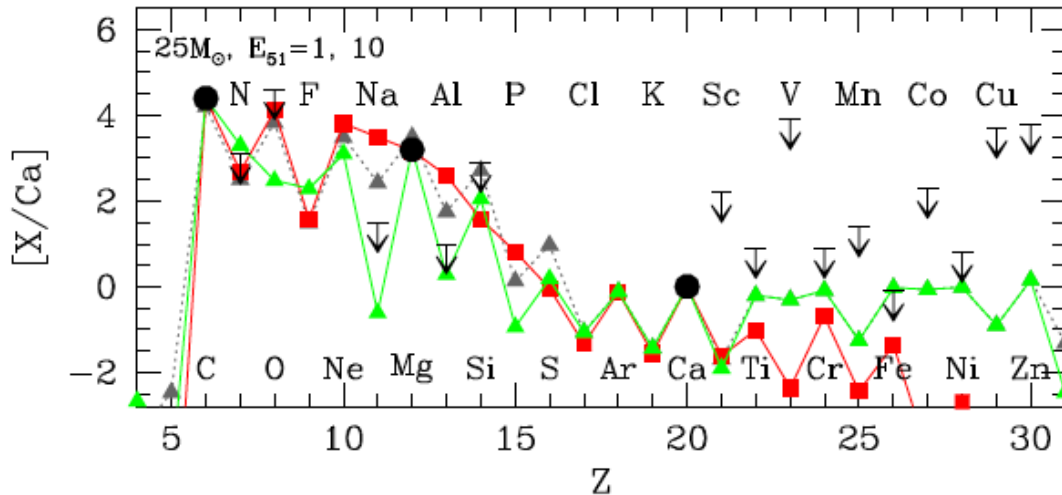


SM 0313-6708 vs.

Pop III SN yields $M=25M_{\odot}$ and $40M_{\odot}$

■: $E_{51}=1$ (supernova)

▲: $E_{51}=10$ (hypernova)



- Extreme C-enhancement: ejection of C in the outer region while fallback of Fe, Ca in the inner region
- Given only C, Mg, Ca abundances it is not possible to distinguish between the 25 and 40 M_{\odot} models

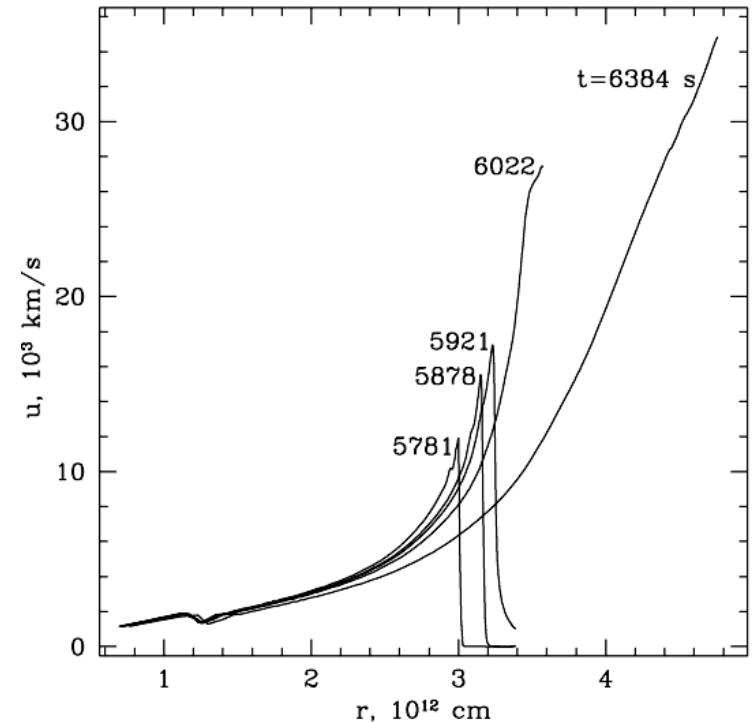
$$[\text{Fe}/\text{H}] = \log_{10} \left(\frac{N_{\text{Fe}}}{N_{\text{H}}} \right)_{\text{star}} - \log_{10} \left(\frac{N_{\text{Fe}}}{N_{\text{H}}} \right)_{\text{sun}}$$

Ishigaki et al. 2014

Numerical algorithms STELLA and RADA

STELLA (Static Eddington-factor Low-velocity Limit Approximation) (Blinnikov et al. 1998)

- 1D Lagrangian Hydro + Radiation Moments Equations, VEF closure, multigroup (100-300 groups, up to 1000), implicit scheme
- Opacity includes photoionization, free-free absorption, lines and electron scattering (Blandford, Payne 1981). Ionization – Saha's approximation
- STELLA was used in modeling of many SN light curves: SN 1987A, SN 1993J and many others (Blinnikov et al. 2006)



- Matter velocity at the epoch of shock breakout versus Eulerian radius r (bottom) in the model for SN 1987A from Blinnikov (1999). The proper time is given near the curves.

Shock breakout. Analytic estimations

Imshennik, Nadëzhin 1988; Matzner McKee 1998

$$(R_0/r - 1) \approx (R_0 - r)/R_0 \equiv x$$

$$\rho = K_1 x^n$$

Self-similar solution (Gandel'man, Frank-Kamenetskii (1956), Sakurai (1960))

$$D = K_2 x_y^{-\lambda}$$

$$\tau_{ye} \approx \frac{c x_{ye}^\lambda}{(\lambda + 1) K_2} = \frac{c}{(\lambda + 1) D_e} \sim \frac{c}{D_e}$$

$$\frac{c}{D_e} \approx \tau_{ye} = \int_{R_{ye}}^{R_0} \kappa \rho dr = \frac{1}{4} K_1 \kappa R_0 x_{ye}^4, \quad x_{ye} = 1 - \frac{R_{ye}}{R_0}$$

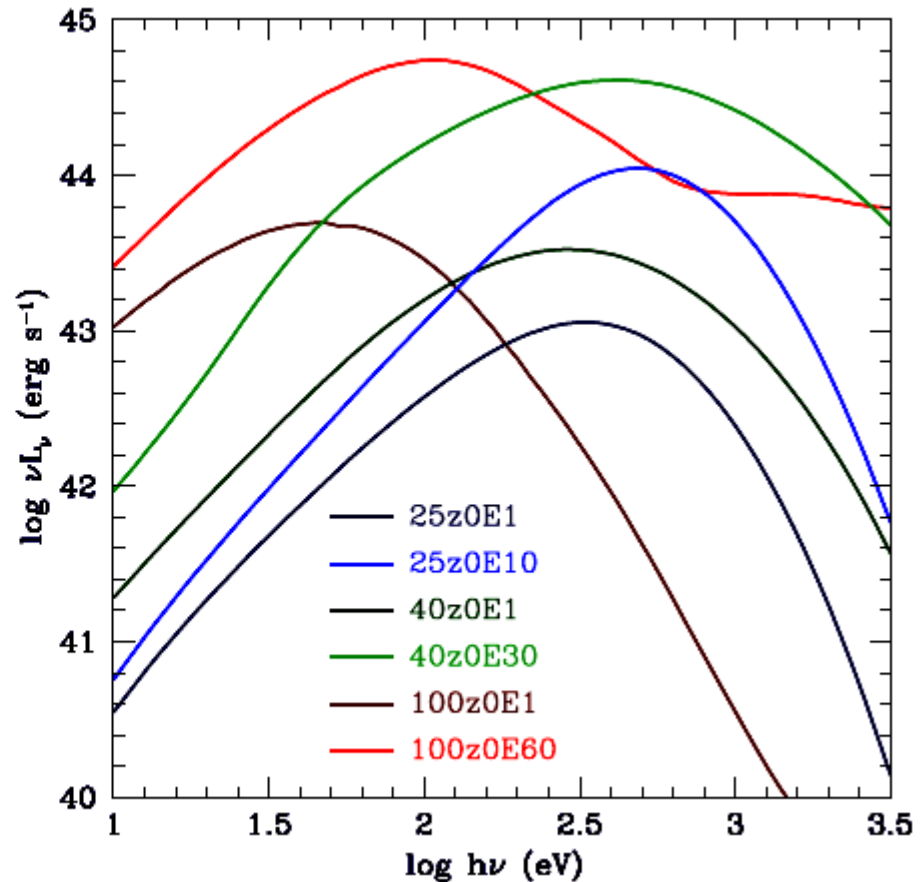
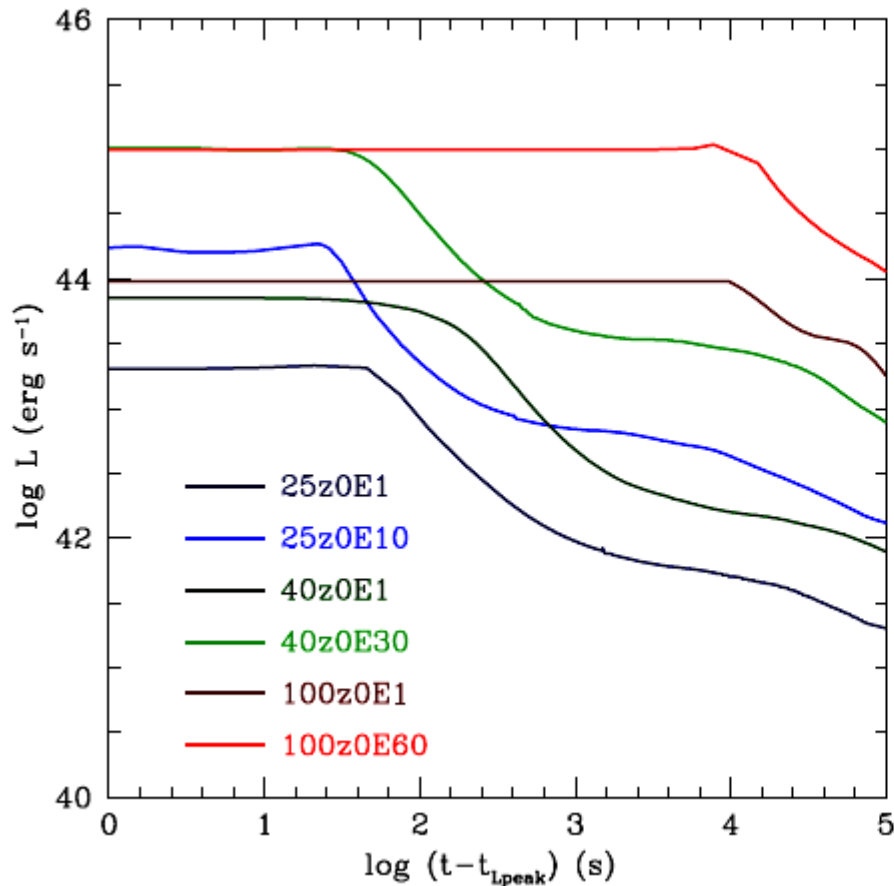
Z0 light curve at shock breakout epoch

$$\Delta t_{SBO} \sim \kappa^{-0.58} E^{-0.79} M^{0.07} R^{1.74} \quad (\text{RSG})$$

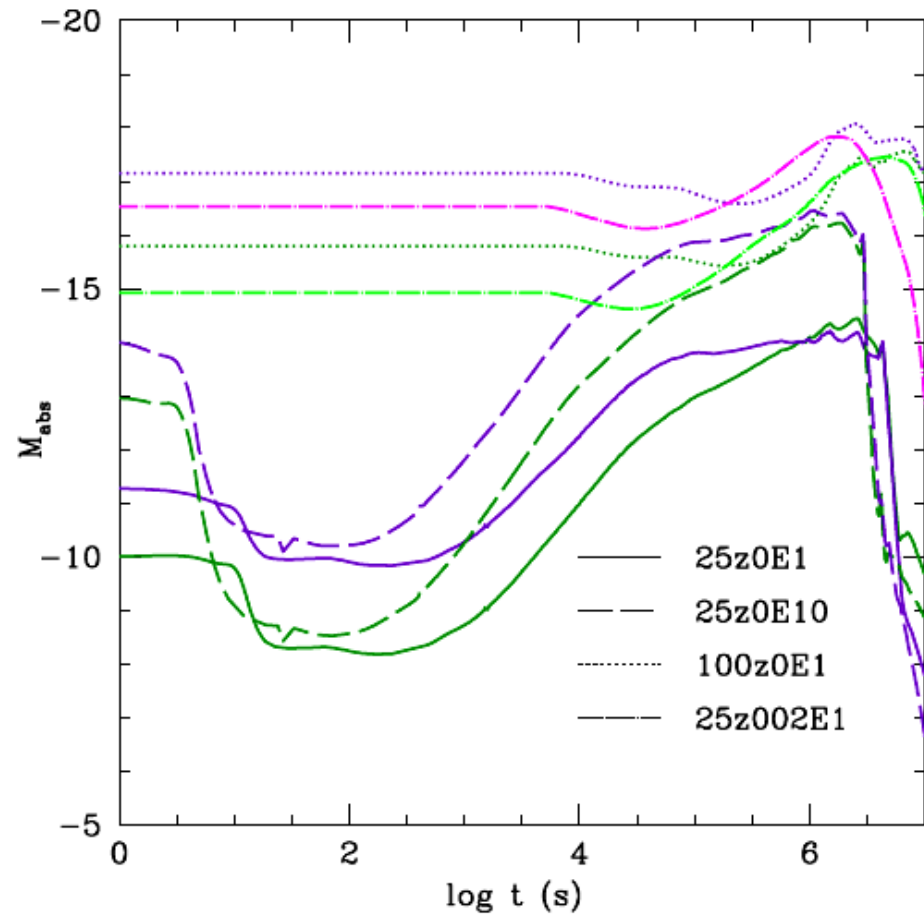
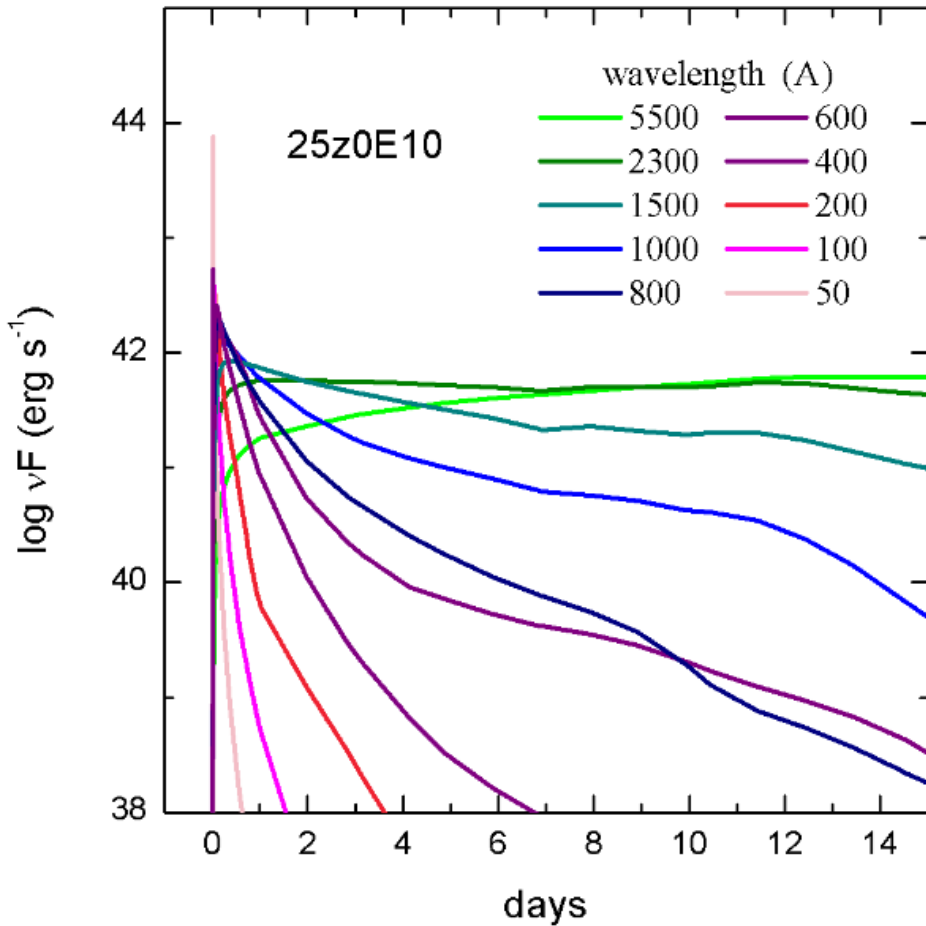
$$\Delta t_{SBO} \sim \kappa^{-0.45} E^{-0.72} M^{-0.09} R^{1.90} \quad (\text{BSG})$$

$$L_{SBO} \sim \kappa^{-0.29} E^{1.35} M^{-0.55} R^{-0.13} \quad (\text{RSG})$$

$$L_{SBO} \sim \kappa^{-0.39} E^{1.30} M^{-0.44} R^{-0.22} \quad (\text{BSG})$$



Z0 light curve at shock breakout epoch



Plateau ant tail phase. Analytic estimations

Litvinova, Nadëzhin 1988; Popov2003

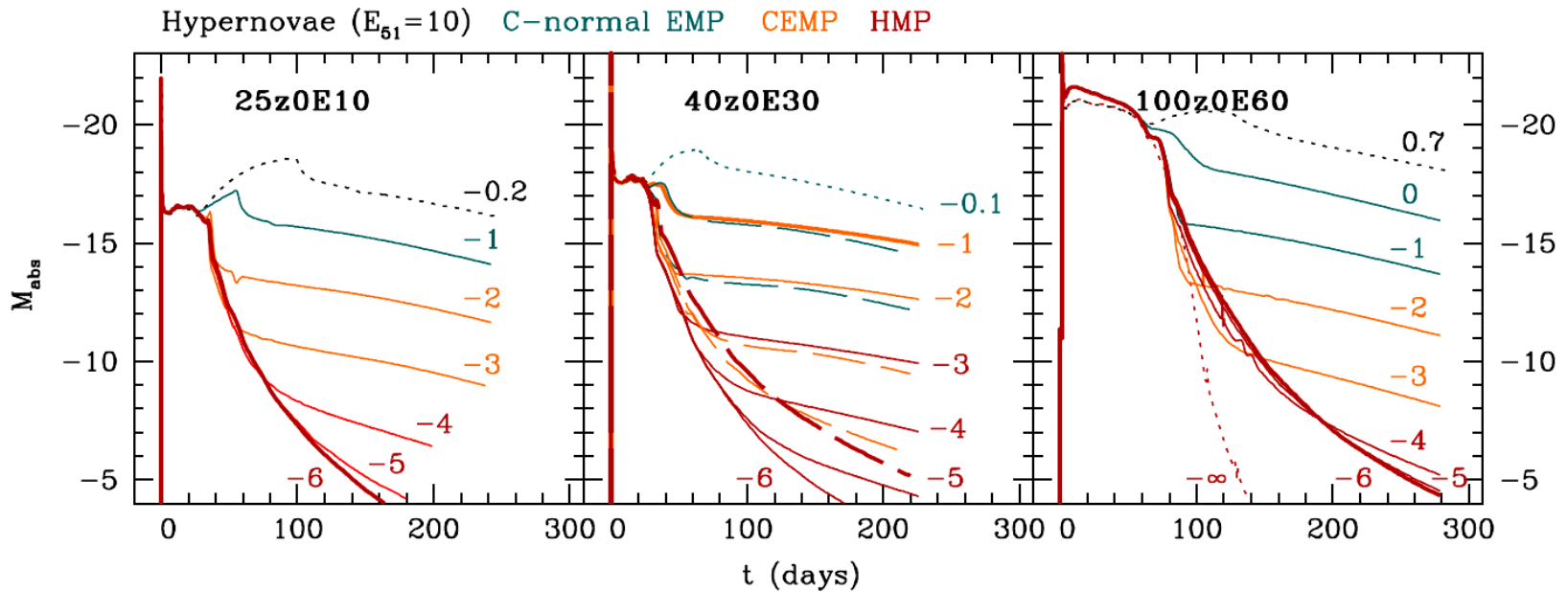
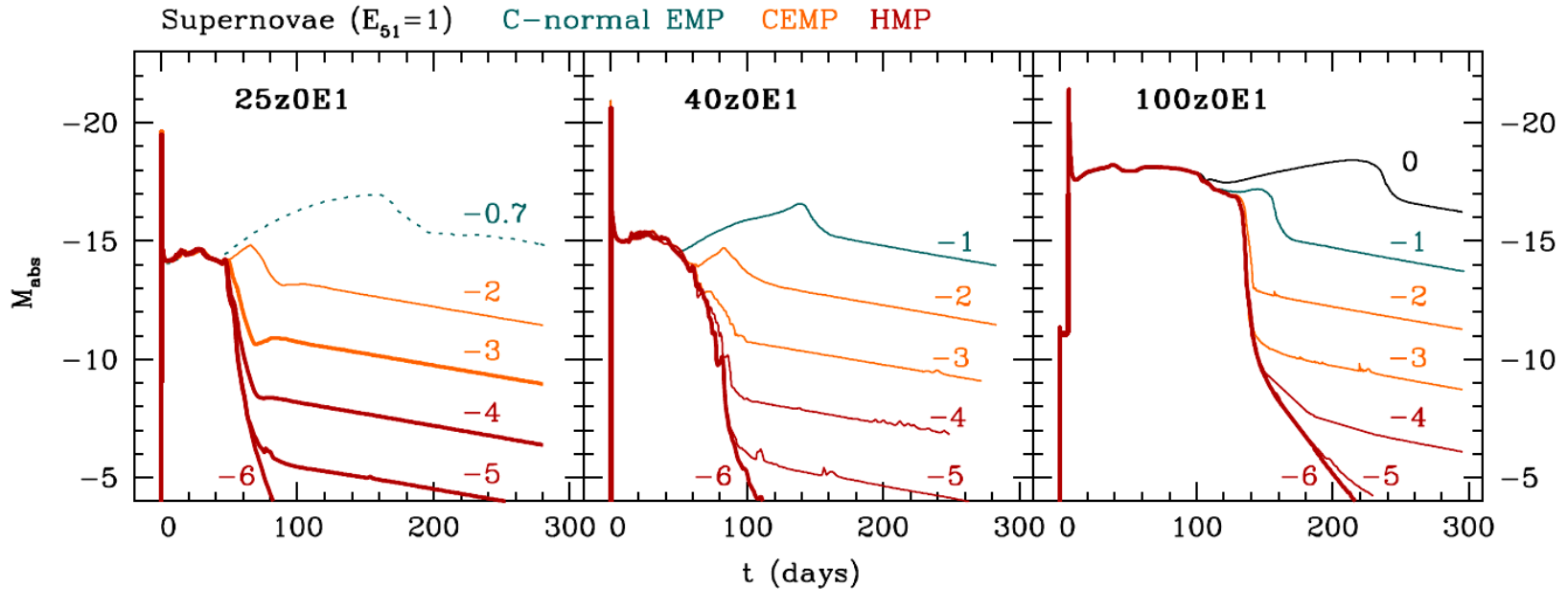
$$\Delta t = -0.191 \lg E + 0.186 \lg R + 0.566 \lg M + 1.047$$

$$V = -2.34 \lg E - 1.80 \lg R + 1.22 \lg M - 11.307$$

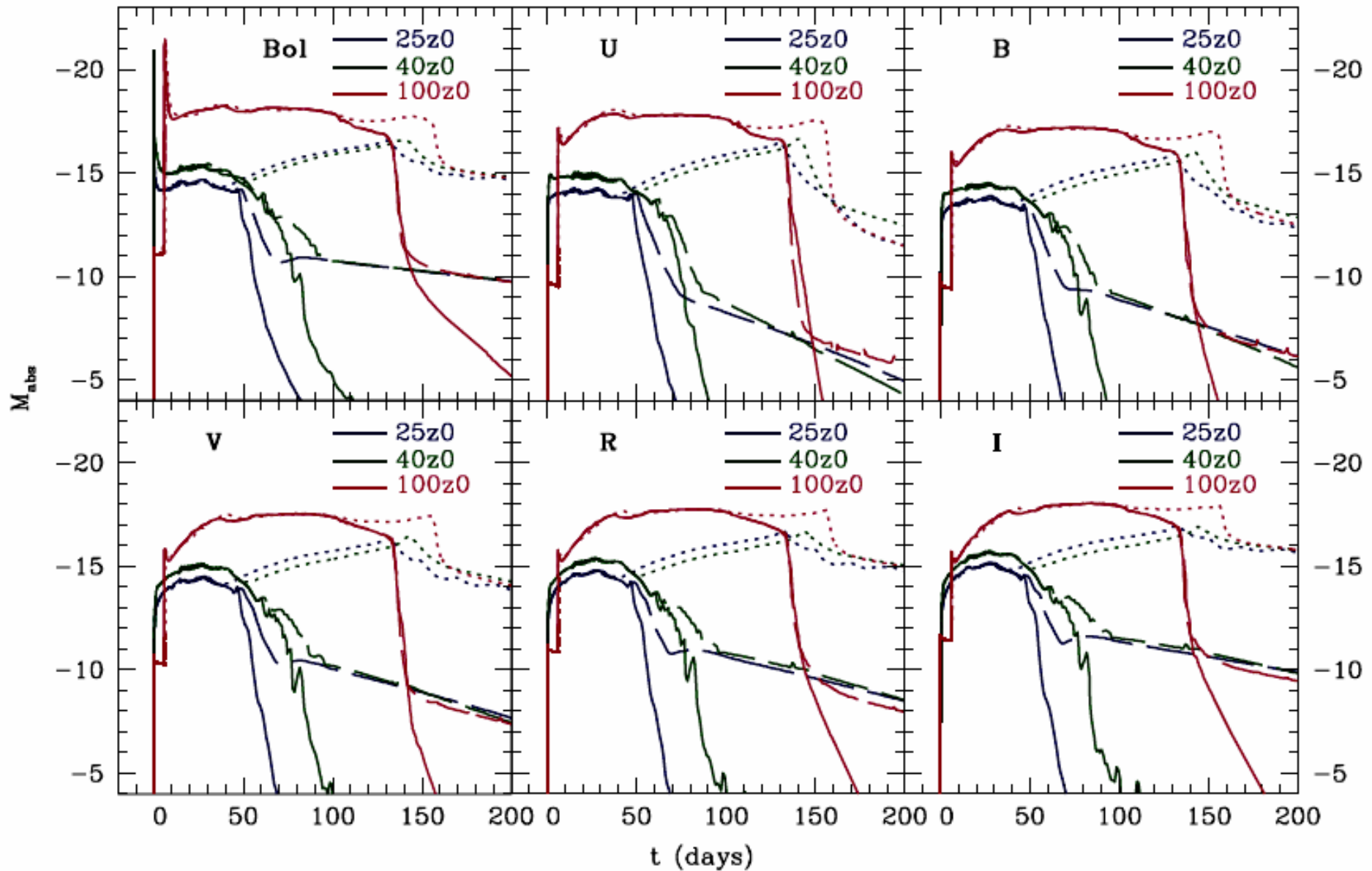
Nadëzhin 1994 (^{56}Co tail):

$$M_{bol} = -19.19 - 2.5 \lg \left(\frac{M_{Ni0}}{M_{\odot}} \right) - 1.09 \frac{t}{\tau_{Co}}$$

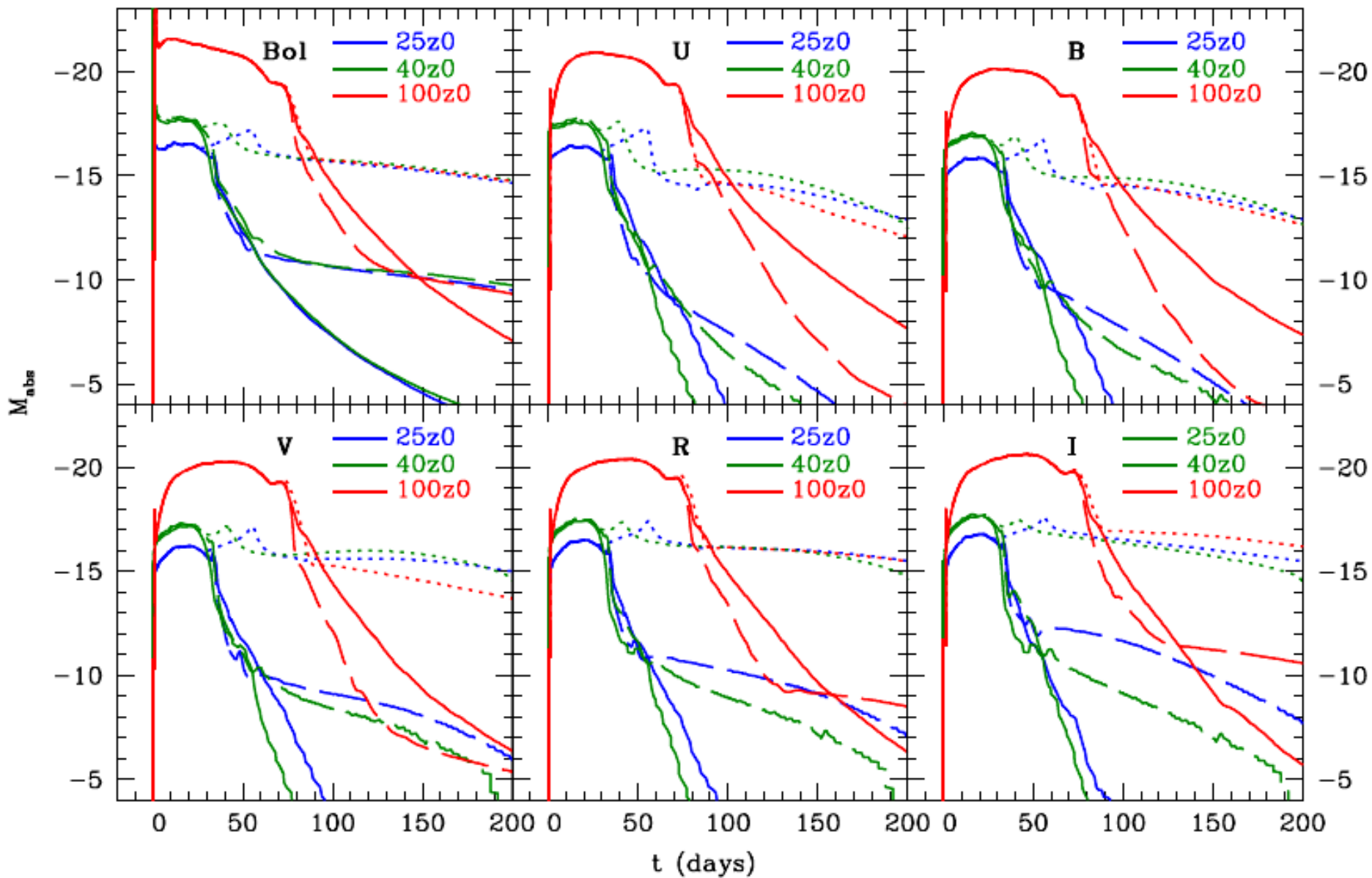
Bolometric light curves of z0 SNe



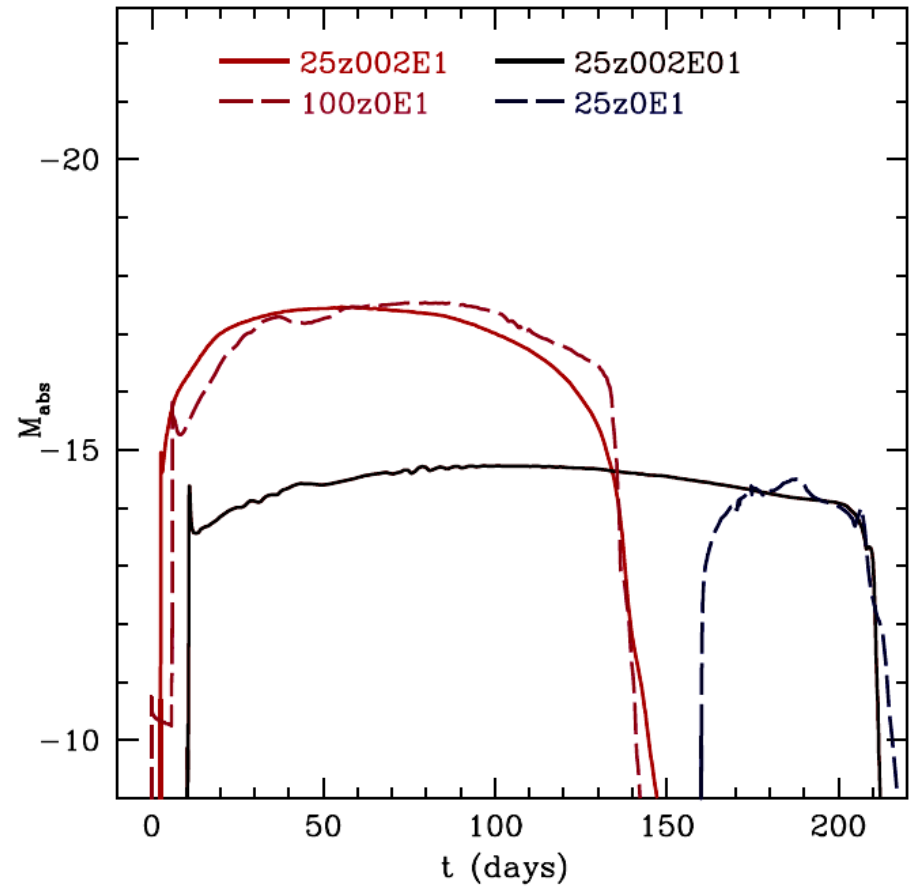
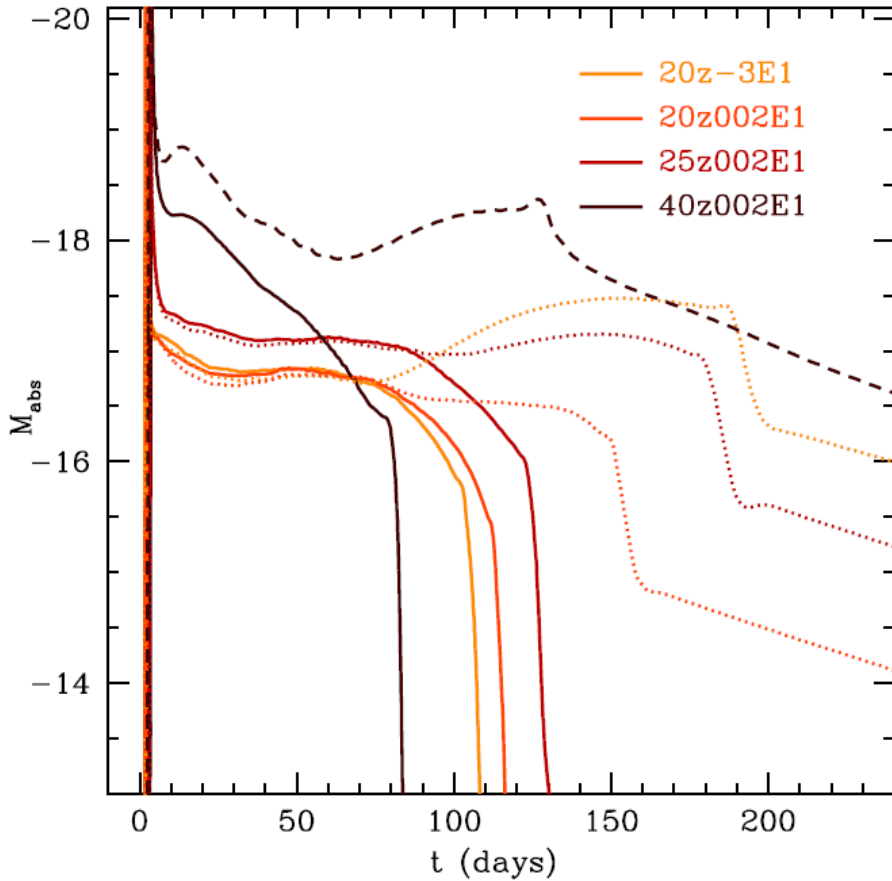
Bolometric and UBVRI light curves of z0 SNe



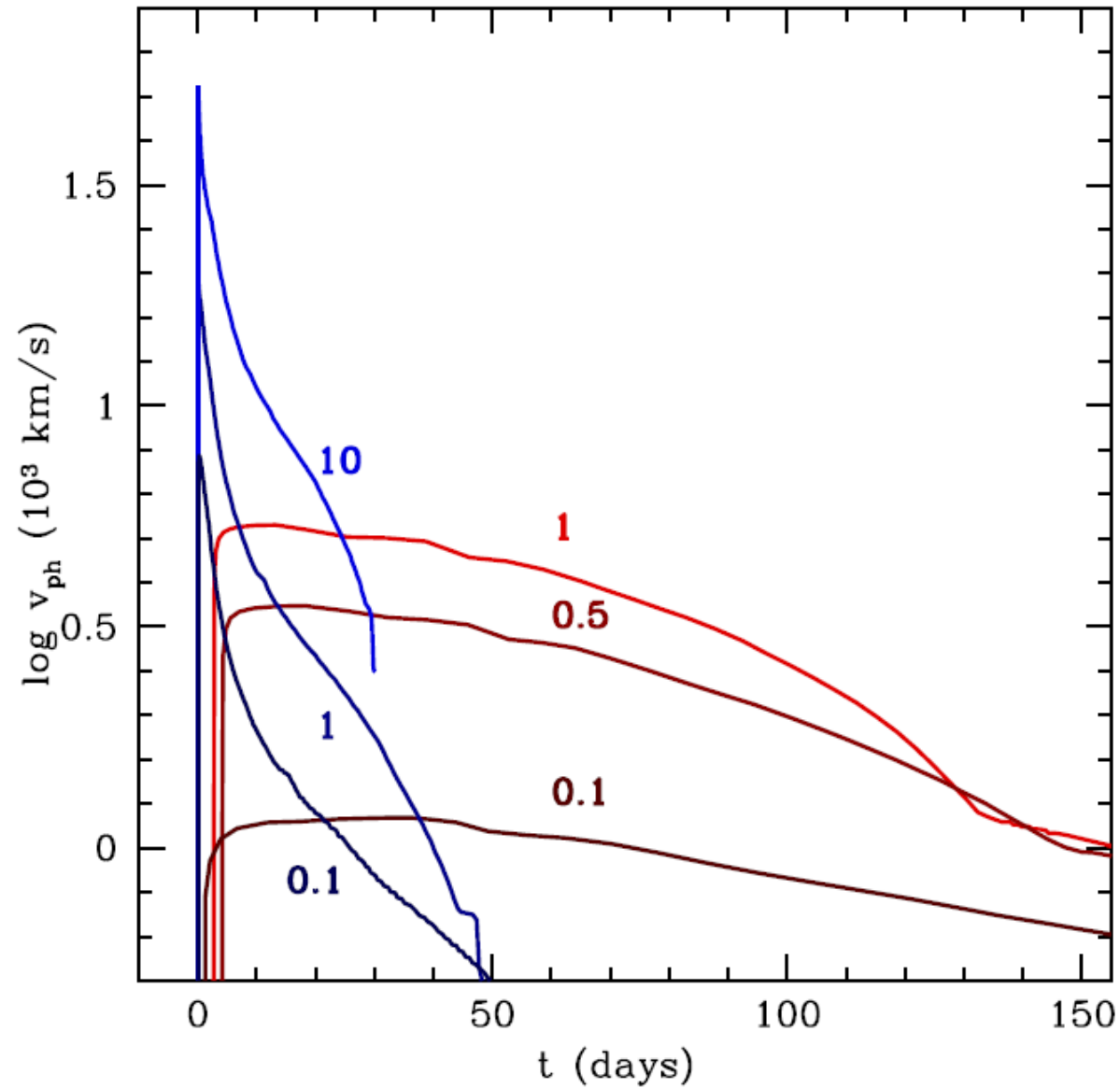
Bolometric and UBVRI light curves of z0 HNe



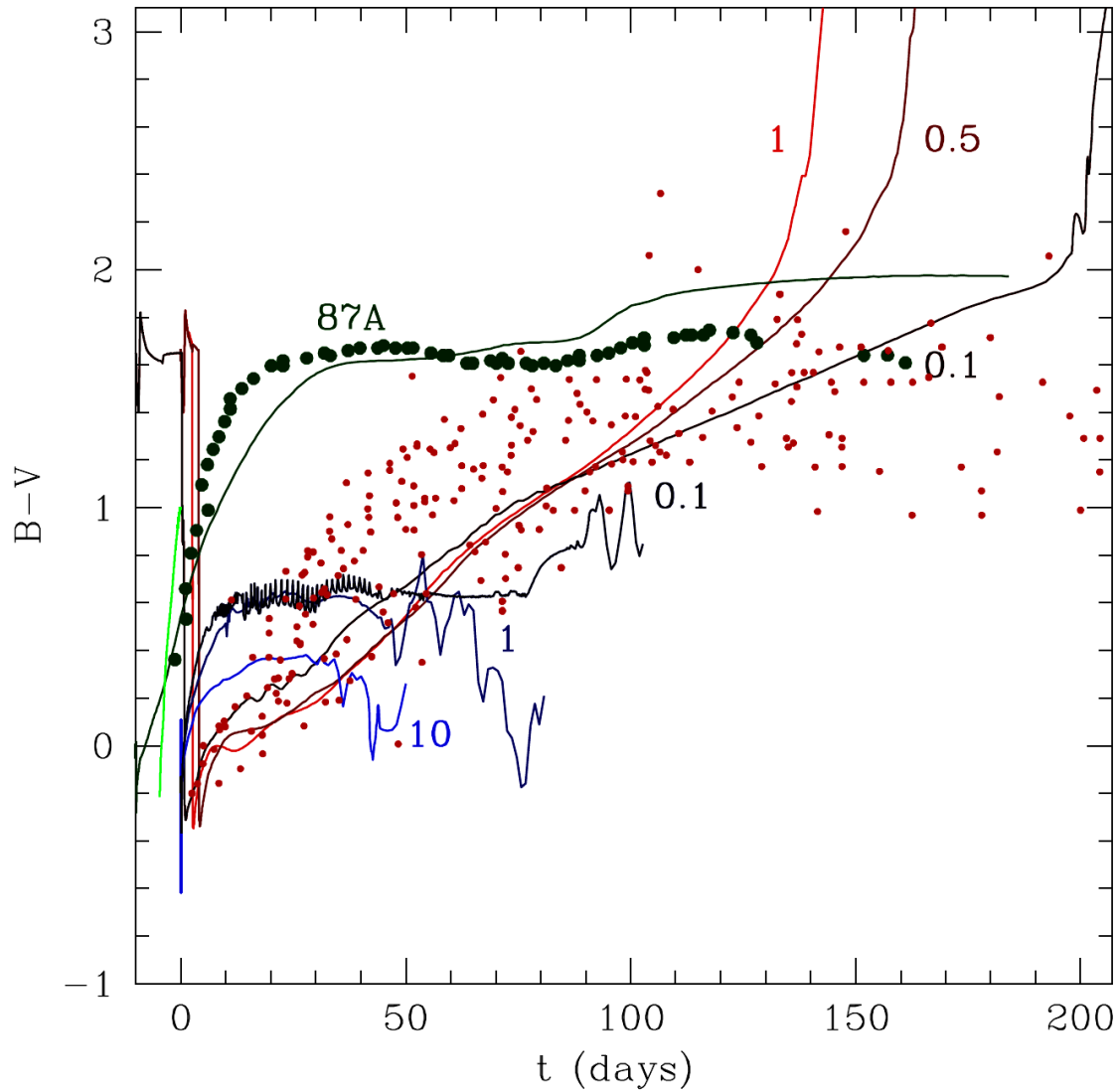
Bolometric and light curves of z002 SNe



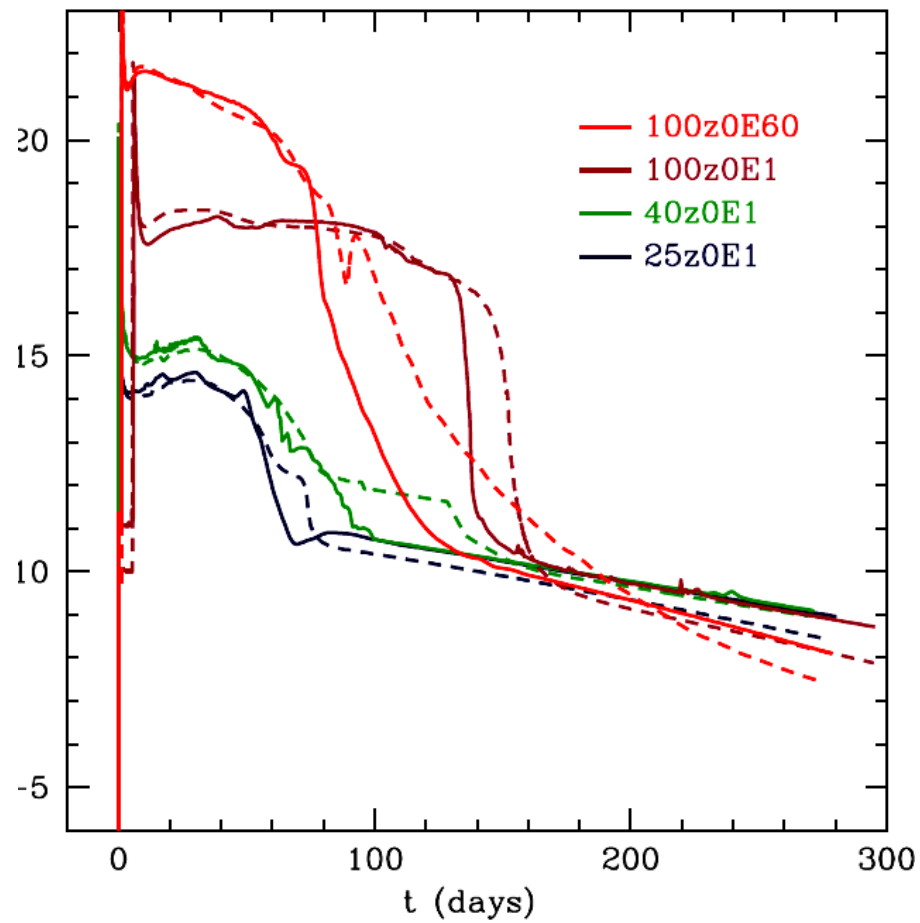
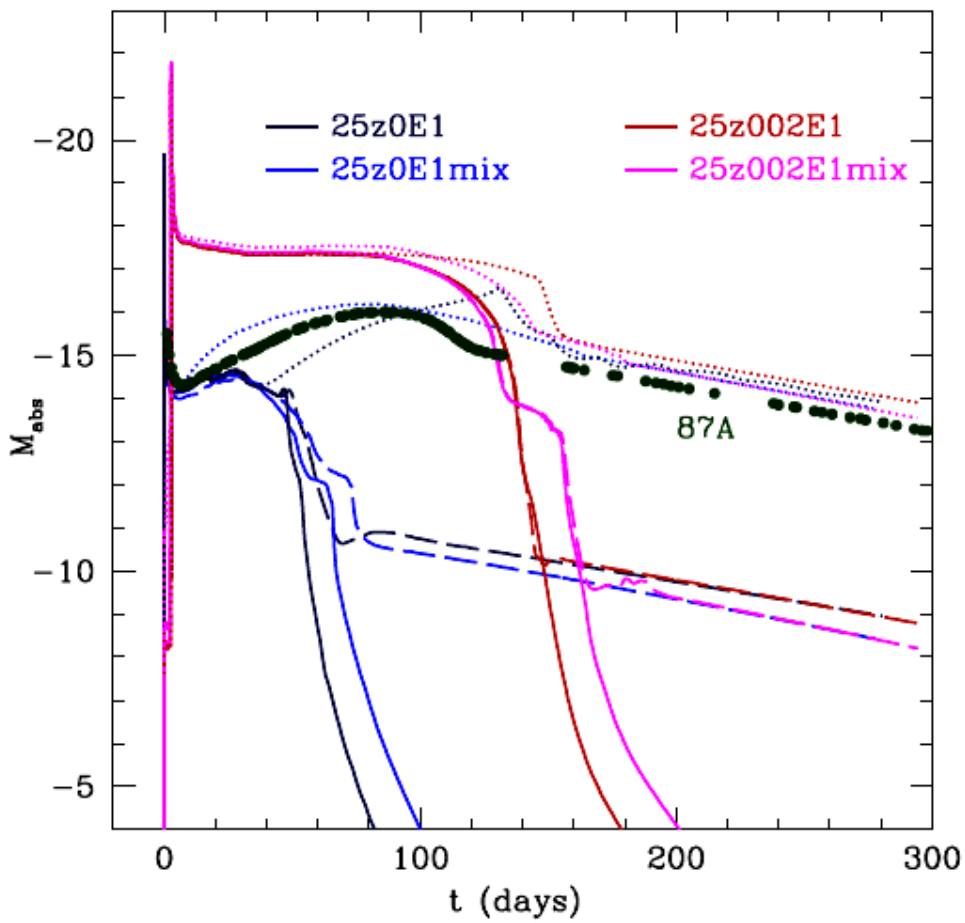
Photospheric velocities, $M=25M_{\odot}$



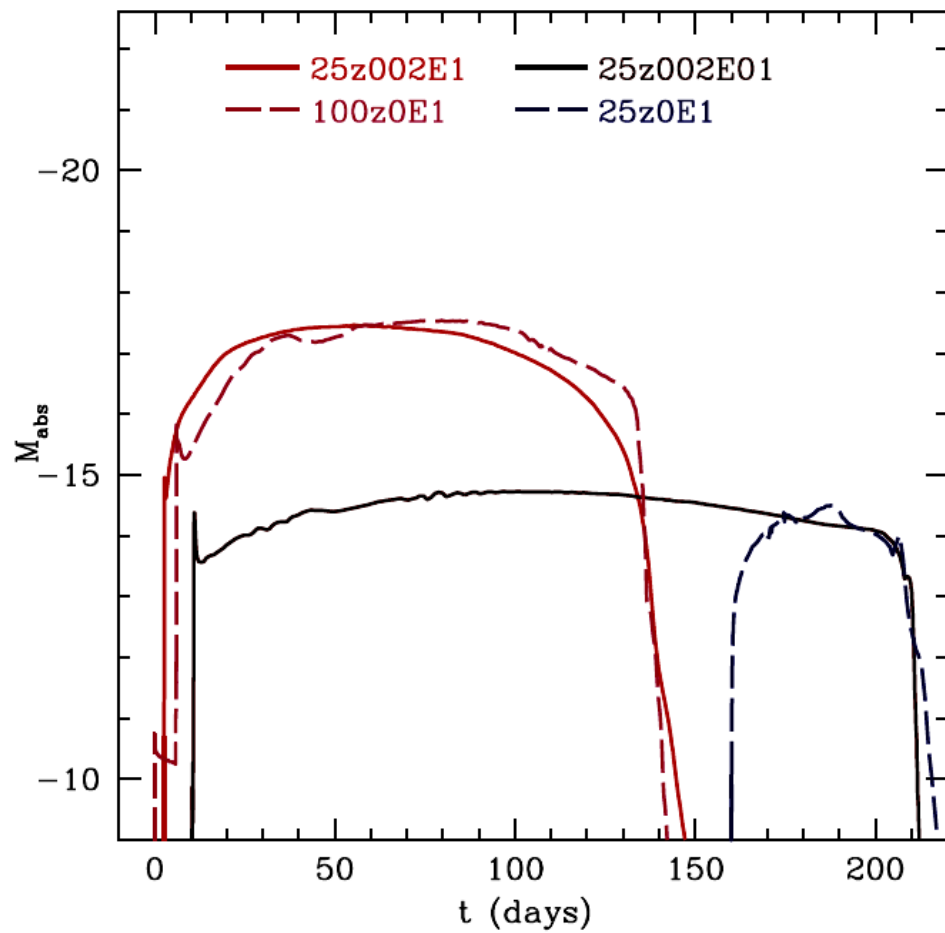
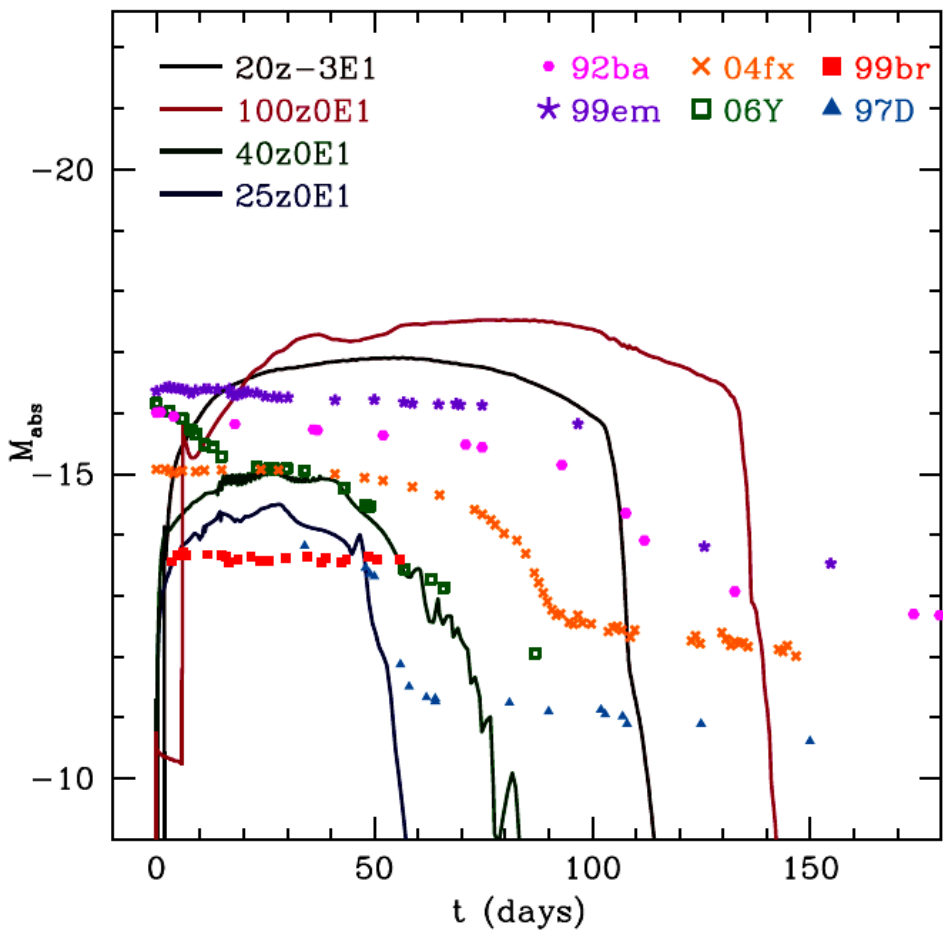
Color evolution curves



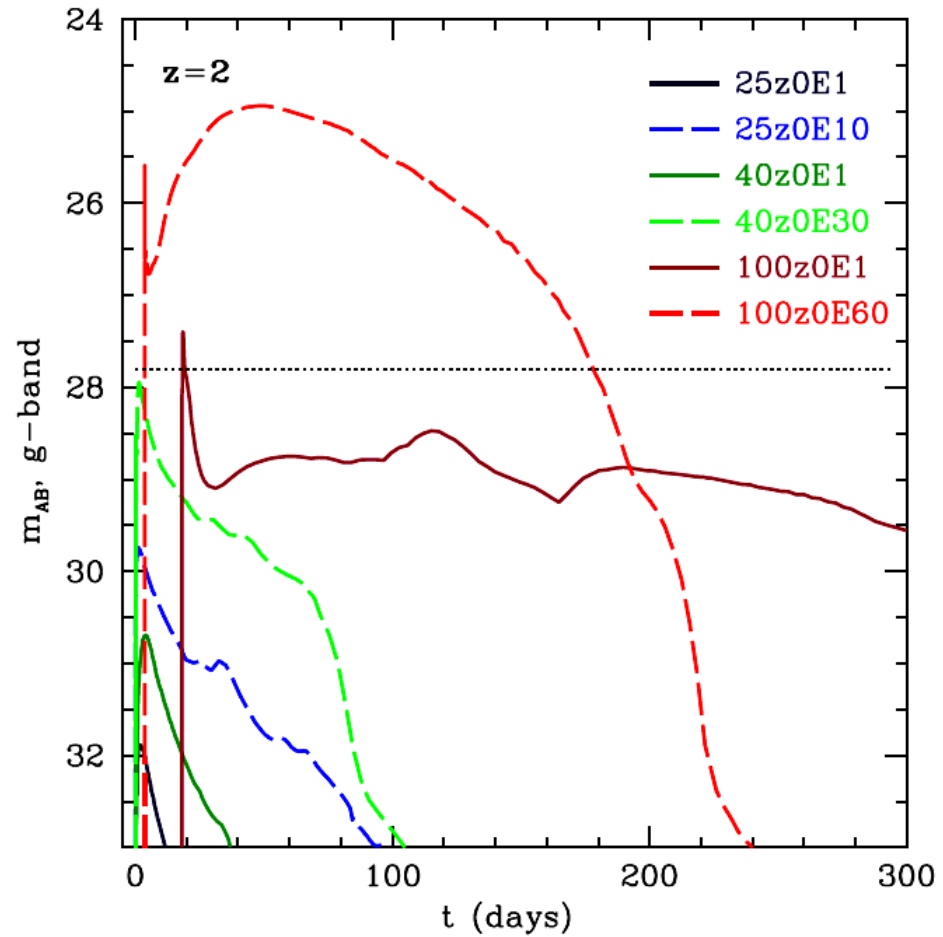
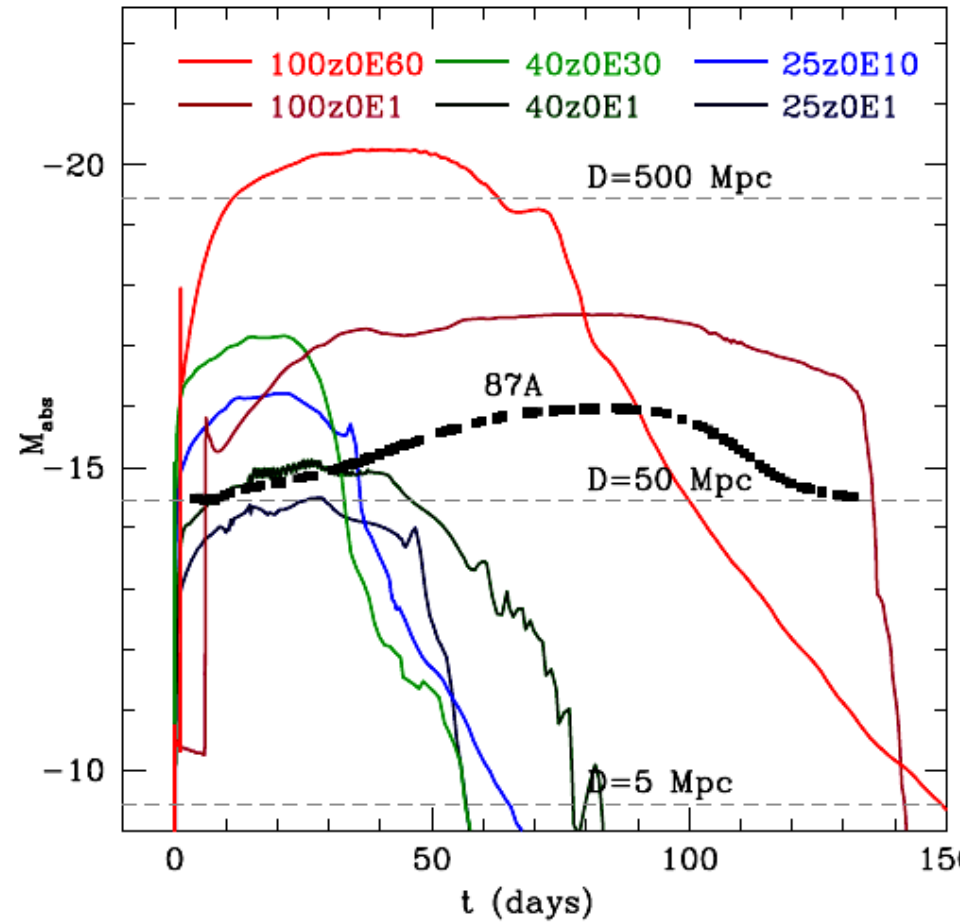
Mixing



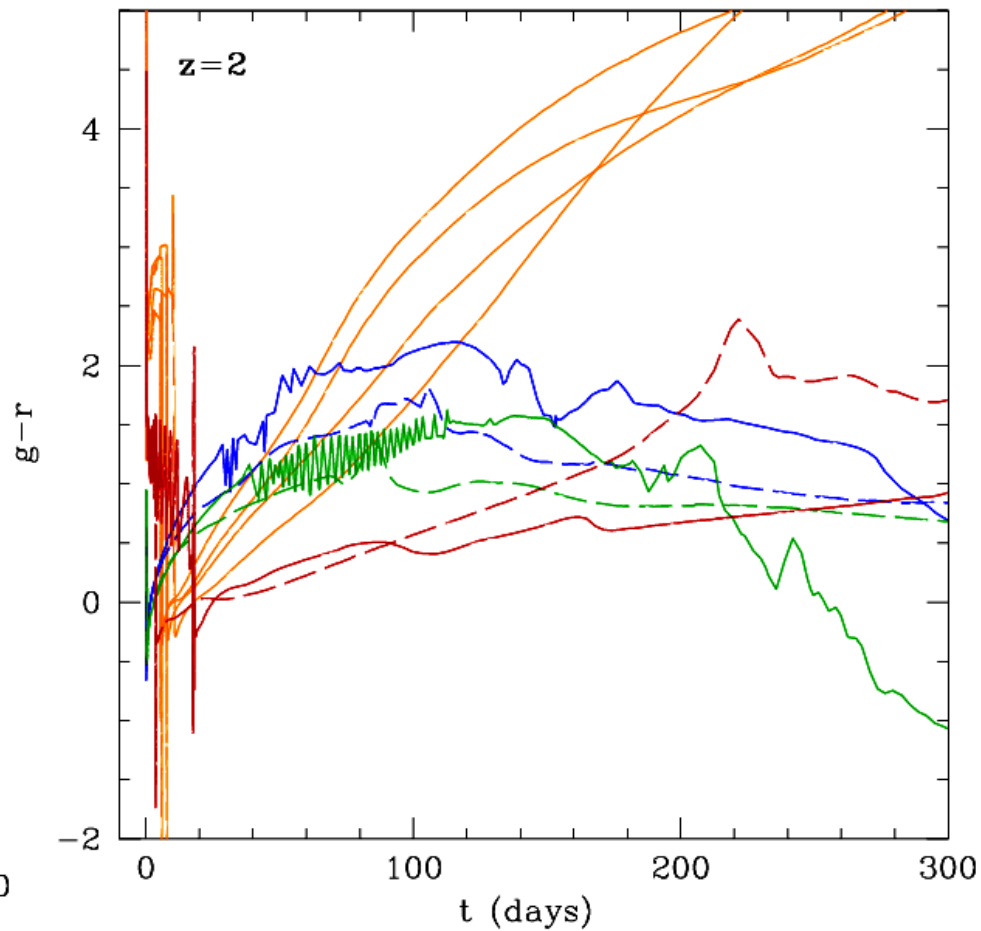
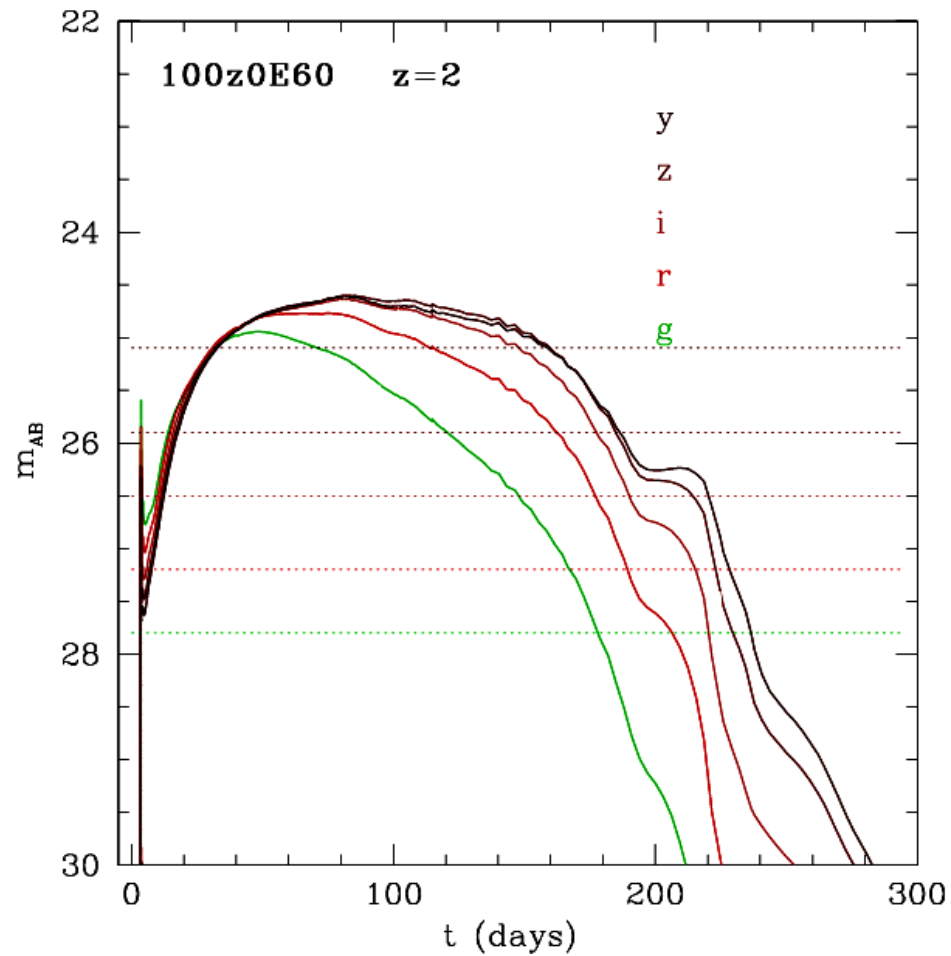
Comparison with observed SNe



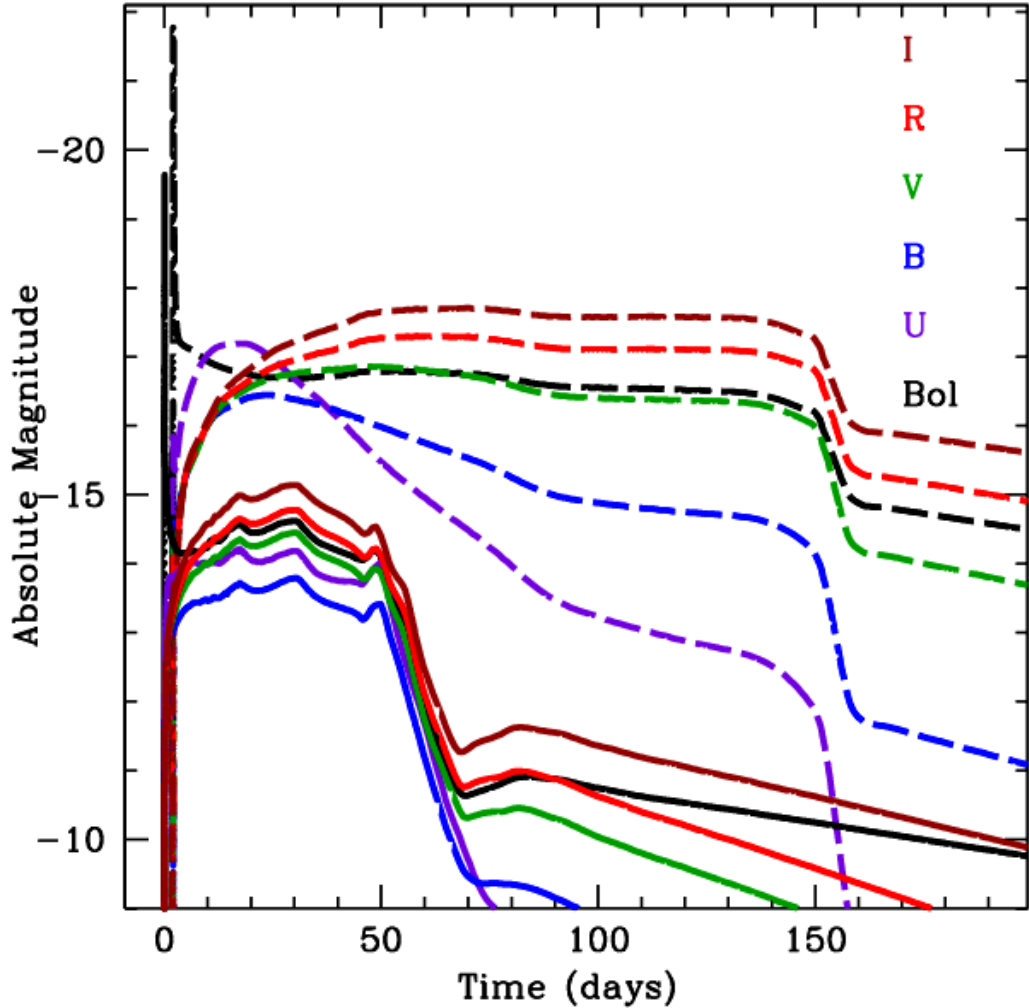
Requirements for observation



Light curves and color evolution curves, $z=2$



Multicolor light curves. Z0 vs solar metallicity



- Bolometric (black line) and UBVRI light curves; zero (solid line), solar (dashed line) metallicity models. $M=25M_{\odot}$, $E_{51}=1$.

Conclusions . Pop III CCSN light curve simulations.

- BSGs are typical presupernovae for Pop III core-collapse SNe with $M_{\text{MS}} \lesssim 40\text{--}60M_{\odot}$.

Shock breakout: shorter duration (100s) and harder UV spectra (0.1–0.3keV) of lower luminosity compared to RSG progenitors.

- The plateau phase is common to both BSG and RSG. The duration of the plateau phase is often unknown from observations. The evolution of the photosphere's velocity is more useful for Pop III identification.

The flat color evolution curve B - V during the plateau phase can be used as an indicator of Pop III and low-metallicity SNe.

Conclusions. Detectability.

- The direct detection of Pop III core-collapse SNe is hardly possible at high redshift (Whalen et al. 2013), but Pop III hypernovae will be visible to the James Webb Space Telescope (JWST) at $z \sim 10\text{--}15$ (Smidt et al. 2014). HSC/Subaru can detect Pop III SNe in metal-free gas pockets ($z \sim 2$).
- The results of our simulations are suitable for identification of low-metallicity supernovae in the nearby universe in galaxies with $Z \sim 10^{-5}\text{--}10^{-4}$.